ANNUAL REVIEWS

Annual Review of Nutrition

Ins and Outs of the TCA Cycle: The Central Role of Anaplerosis

Melissa Inigo,[1] Stanisław Deja,[1,2] and Shawn C. Burgess[1,3]

[1]Center for Human Nutrition, University of Texas Southwestern Medical Center, Dallas, Texas 75390, USA; email: shawn.burgess@utsouthwestern.edu

[2]Department of Biochemistry, University of Texas Southwestern Medical Center, Dallas, Texas 75390, USA

[3]Department of Pharmacology, University of Texas Southwestern Medical Center, Dallas, Texas 75390, USA

Annu. Rev. Nutr. 2021. 41:19–47

First published as a Review in Advance on July 16, 2021

The *Annual Review of Nutrition* is online at nutr.annualreviews.org

https://doi.org/10.1146/annurev-nutr-120420-025558

Keywords

anaplerosis, cataplerosis, TCA cycle, pyruvate cycling, gluconeogenesis, lipogenesis

Abstract

The reactions of the tricarboxylic acid (TCA) cycle allow the controlled combustion of fat and carbohydrate. In principle, TCA cycle intermediates are regenerated on every turn and can facilitate the oxidation of an infinite number of nutrient molecules. However, TCA cycle intermediates can be lost to cataplerotic pathways that provide precursors for biosynthesis, and they must be replaced by anaplerotic pathways that regenerate these intermediates. Together, anaplerosis and cataplerosis help regulate rates of biosynthesis by dictating precursor supply, and they play underappreciated roles in catabolism and cellular energy status. They facilitate recycling pathways and nitrogen trafficking necessary for catabolism, and they influence redox state and oxidative capacity by altering TCA cycle intermediate concentrations. These functions vary widely by tissue and play emerging roles in disease. This article reviews the roles of anaplerosis and cataplerosis in various tissues and discusses how they alter carbon transitions, and highlights their contribution to mechanisms of disease.

Contents

1. INTRODUCTION 20
   1.1. Background 20
   1.2. Definitions and Nuances 21
2. MAPPING TCA CYCLE METABOLISM 22
   2.1. Carbon Transitions of the TCA Cycle and Anaplerosis 22
   2.2. Tracer and Isotopomer Approaches 24
   2.3. Label Recycling 25
3. PATHWAYS OF CATAPLEROSIS AND ANAPLEROSIS IN BIOSYNTHESIS 26
   3.1. Hepatic Gluconeogenesis 26
   3.2. Extrahepatic Gluconeogenesis 30
   3.3. Lipogenic Tissue 31
   3.4. Central Nervous System 31
   3.5. Porphyrin Synthesis 32
4. CATABOLIC FUNCTIONS OF ANAPLEROSIS AND CATAPLEROSIS 33
   4.1. Anaplerotic Substrate REcycling 33
   4.2. Nitrogen Trafficking 33
   4.3. Heart 36
   4.4. Energetics and Redox 37
5. ADAPTIVE ROLES OF ANAPLEROSIS AND CATAPLEROSIS IN CANCER 37
6. SUMMARY 38

1. INTRODUCTION

1.1. Background

Over the past 2 decades, our view of the mitochondrion as a site of cellular respiration has broadened to include essential roles in biosynthesis, growth, redox regulation, and cell signaling. Many of the metabolites necessary for these functions are derived from the tricarboxylic acid (TCA) cycle. The eight intermediates of the TCA cycle, and the enzymes that link them, form an elegant system of oxidative decarboxylation that facilitates the controlled combustion of nutrients. The TCA cycle intermediate oxaloacetate (OAA) condenses with acetyl-CoA to generate citrate, and seven subsequent reactions produce two CO_2 molecules, four reducing equivalents ($NADH/FADH_2$), and a GTP and, importantly, regenerate OAA. In principle, a finite number of TCA cycle intermediates can facilitate the oxidation of an infinite number of nutrient molecules. However, most of the organic acids of this system are also substrates for biochemical reactions outside of mitochondria, and once they are lost, they must be replaced. The phrase "anaplerotic sequence" was used by Hans Kornberg to describe this process. He noted that for the

> proper description of the flow of nutrients associated with the release of energy and its utilization for biosyntheses, a special type of metabolic pathway must operate inside the cell which may be regarded as serving solely to maintain the functioning of the tricarboxylic acid cycle and other amphibolic routes. It has been proposed to generically designate this type of ancillary pathway as an anaplerotic sequence. (72, p. 565)

Kornberg showed that, in the absence of an anaplerotic pathway, TCA cycle function declines and cell replication ceases. The emerging view of mitochondrial function in cell proliferation, biosynthesis, and cell signaling was predicted by Kornberg's (71) research.

1.2. Definitions and Nuances

Anaplerosis perfectly balances pathways that consume TCA cycle intermediates. These pathways, collectively termed cataplerosis, supply substrate for the synthesis of carbohydrates, fats, amino acids, proteins, hormones, nucleotides, and other classes of biomolecules (106) (**Figure 1**). Yet, it is not necessarily obvious what constitutes an anaplerotic and/or cataplerotic sequence. By

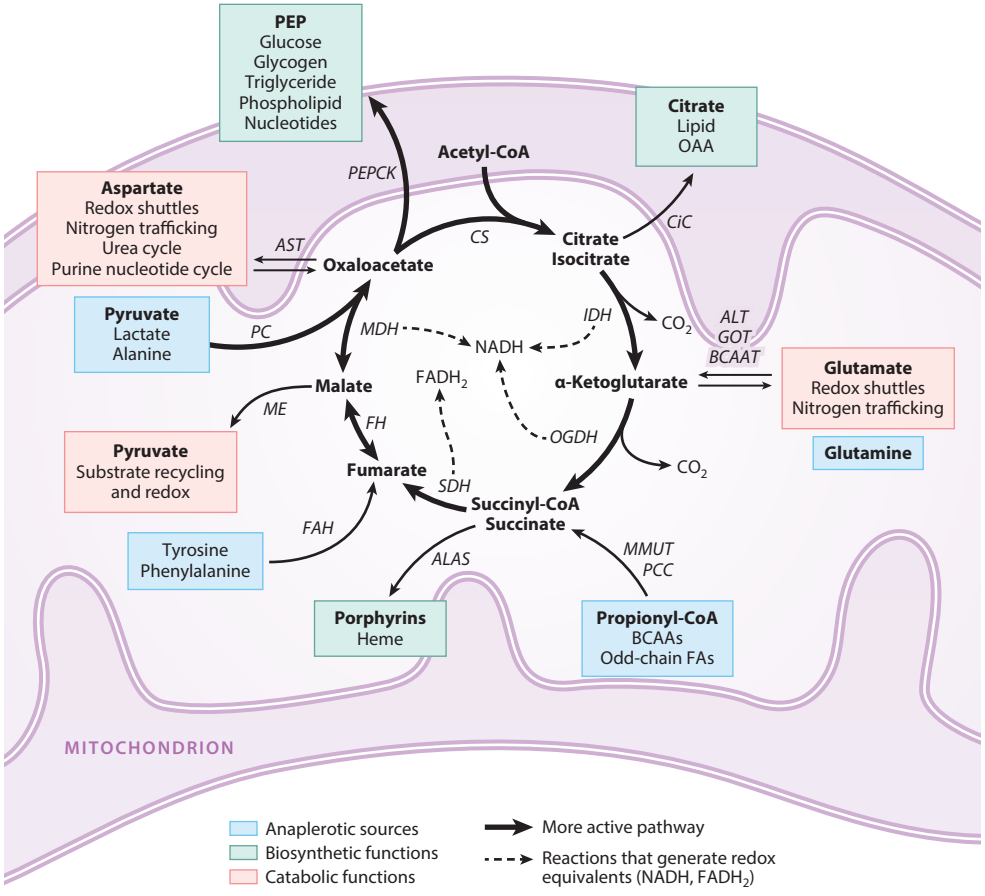

Figure 1

Anaplerosis and cataplerosis link the TCA cycle to biosynthesis and catabolism. Abbreviations: *ALAS*, δ-aminolevulinic acid synthase; *ALT*, alanine aminotransferase; *AST*, aspartate aminotransferase; BCAAs, branched-chain amino acids; *BCAAT*, branched-chain amino acid aminotransferase; *CiC*, citrate-isocitrate carrier; *CS*, citrate synthase; *FAH*, fumarylacetoacetate hydrolase; FAs, fatty acids; *FH*, fumarate hydratase; *GOT*, glutamic-oxaloacetic transaminase; *IDH*, isocitrate dehydrogenase; *MDH*, malate dehydrogenase; *ME*, malic enzyme; *MMUT*, methylmalonyl-CoA mutase; OAA, oxaloacetate; *OGDH*, 2-oxoglutarate dehydrogenase (or α-ketoglutarate dehydrogenase); *PC*, pyruvate carboxylase; *PCC*, propionyl-CoA carboxylase; PEP, phosphoenolpyruvate; *PEPCK*, phosphoenolpyruvate carboxykinase; redox, reduction–oxidation; *SDH*, succinate dehydrogenase; TCA, tricarboxylic acid.

Kornberg's strict definition, one could argue that cataplerosis and the need for anaplerosis only occur when a TCA cycle intermediate is lost to biosynthesis. For instance, the liver uses OAA as a substrate for glucose synthesis; thus, an equally active anaplerotic sequence converts pyruvate to OAA. This example illustrates the net loss of an OAA to biosynthesis and its replacement by a new OAA. Yet, the terms anaplerotic and cataplerotic are often applied more broadly. Citrate transport, which provides an essential source of cytosolic acetyl-CoA for lipid synthesis, is classically considered a cataplerotic pathway (106). However, if the same OAA carbons cleaved by the citrate lyase reaction are subsequently returned to mitochondria, one might argue that no net loss or gain of TCA cycle carbon mass has transpired. Kornberg's definition leaves room for interpretation: Anaplerosis serves "solely to maintain the function of the tricarboxylic acid cycle and other amphibolic routes." In other words, any pathway that contributes intermediates to the TCA cycle, other than the synthesis of citrate from OAA and acetyl-CoA, is usually considered anaplerotic. Likewise, any pathway that removes carbon from the TCA cycle, other than CO_2, is usually considered cataplerotic. Such a broad definition includes futile cycles, redox shuttles, and catabolic pathways of amino acid metabolism and nitrogen trafficking (**Figure 1**).

This article reviews the roles of anaplerotic and cataplerotic pathways in metabolism and attempts to put them in context with emerging concepts in molecular metabolism. We cover the molecular transitions that define these pathways and allow them to be detected by tracer approaches. We describe the biochemical routes of anaplerosis and cataplerosis and how these pathways allow mitochondria to mediate anabolic and catabolic processes. Finally, we discuss these pathways in the context of the tissues where they are most active and the roles they play in a variety of diseases.

2. MAPPING TCA CYCLE METABOLISM

> . . .for they took away the old planks as they decayed, putting in new and stronger timber in their places, insomuch that this ship became a standing example among the philosophers, for the logical question of things that grow; one side holding that the ship remained the same, and the other contending that it was not the same.
>
> —Plutarch, *Theseus*

2.1. Carbon Transitions of the TCA Cycle and Anaplerosis

Gluconeogenesis is an archetypal cataplerotic pathway whose high flux and clear relevance to human physiology made it an early target of isotope tracer approaches. Krebs and colleagues (73) observed that lactate was quantitatively converted to glucose by mass balance, but that glucose generated from ^{14}C-lactate was missing 60% of the label, the balance of which was detected as $^{14}CO_2$. The explanation for this observation had come years earlier, when Strisower et al. (128) developed a model to explain how ^{14}C-acetate, a substrate that cannot be used to produce glucose by mass balance, nonetheless generated ^{14}C-glucose. These early experiments established the molecular connections among anaplerosis, TCA cycle intermediates, and cataplerosis required for gluconeogenesis. Over the next 50 years, scientists still struggling to obtain accurate ^{13}C-tracer measurements of gluconeogenesis developed quantitative models to describe anaplerosis and the carbon transitions of the TCA cycle that account for tracer dilution (14, 31, 48, 67, 68, 79). An additional benefit was that these models, and the experiments used to test them, provided a foundation for understanding the carbon transitions of anaplerosis, TCA cycle metabolism, and cataplerosis in general contexts (3, 5, 7, 103, 125, 148).

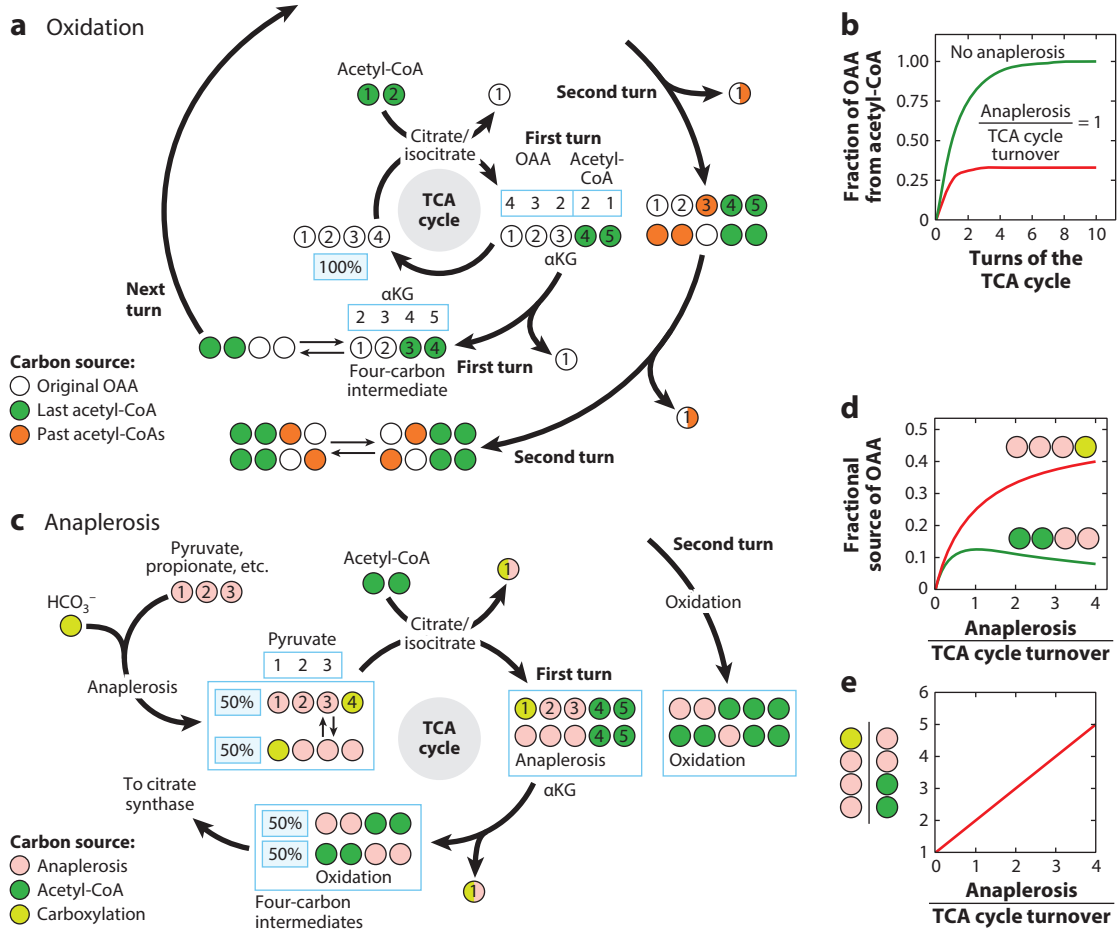

Figure 2

(*a*) Rearrangements of acetyl-CoA atoms during the first and second turns of the TCA cycle are predictable and can be modeled. (*b*) Effect of anaplerosis on acetyl-CoA carbon incorporation into the TCA cycle. The fraction of OAA carbons derived from acetyl-CoA in the absence of anaplerosis (*green line*) during successive turns of the TCA cycle approaches 1 by 10 turns of the cycle. When anaplerosis is active, for example, when the rate of anaplerosis equals the rate of oxidation (*red line*), the fraction of OAA carbons derived from acetyl-CoA will never reach 1 during TCA cycle turnover. Note that the exact kinetics of the process depends on intermediate pool sizes. (*c*) Anaplerosis alters the carbon-atom transitions of the TCA cycle. (*d*) The fractions of OAA derived from anaplerosis (*red line*) and from acetyl-CoA oxidation (*green line*) are dependent on the relative rates of anaplerosis and TCA cycle flux. (*e*) The ratio of these isotopomers is proportional to the ratio of anaplerosis and TCA cycle flux. Abbreviations: OAA, oxaloacetate; TCA, tricarboxylic acid; αKG, α-ketoglutarate.

During the oxidation of acetyl-CoA, its two carbons are condensed with OAA in the citrate synthase reaction to form citrate. The former carbon 1 (C1) of OAA is lost at the isocitrate dehydrogenase (IDH) reaction, and the former C4 of OAA [now C1 of α-ketoglutarate (αKG)] is lost at the 2-oxoglutarate dehydrogenase (or α-ketoglutarate dehydrogenase) (OGDH) reaction. Thus, in the first four reactions of the TCA cycle, two carbons are gained and two different carbons are lost (**Figure 2*a***). C1 and C2 of acetyl-CoA are retained as C5 and C4 of αKG and subsequently become C4 and C3 of succinyl-CoA. An important factor in the carbon transitions of the TCA cycle is that succinate and fumarate intermediates are symmetrical, resulting in C1 and C2 being

indistinguishable from C4 and C3. Thus, when OAA is regenerated at the end of one turn of the cycle, two of its carbons originate from the last acetyl-CoA, with an equal probability of them existing in C1 and C2 or C4 and C3 (**Figure 2*a***). Each turn gradually replaces the carbons of the TCA cycle without introducing new molecules. An OAA molecule will have replaced most of its carbons after traversing the cycle twice, and virtually all after ~10 times (**Figure 2*b***). Like the planks of Theseus's ship, the individual intermediates continue to exist, though all their atoms have been replaced.

Anaplerotic and cataplerotic activity introduce new intermediates into the TCA cycle which prevent the carbons of its intermediates from being completely replaced by acetyl-CoA carbons (**Figure 2*b***). For example, anaplerotic substrates that undergo carboxylation will generate new OAA. C1, C2, and C3 of the new OAA will have originated from the respective carbons of the anaplerotic substrate, while C4 originates from the carboxylation of an endogenous bicarbonate. Rapid reverse equilibration among OAA, malate, and fumarate (i.e., backward scrambling) ensures the symmetry of these sources in four-carbon intermediates (**Figure 2*c***). To the extent that the cycle operates in the oxidative direction, these new OAA carbons will be transmitted to C1, C2, and C3 of αKG as described above. Upon reforming OAA, either C3 and C4 or C1 and C2 are replaced by carbons of acetyl-CoA (**Figure 2*d***). Thus, the carbons of an anaplerotic substrate are interrupted by acetyl-CoA carbons. These carbon transitions have been rigorously described using mathematical models (3, 5, 7, 103, 125, 148).

2.2. Tracer and Isotopomer Approaches

Any ^{13}C tracer that enters the TCA cycle will undergo the carbon transitions of anaplerotic, cataplerotic, and oxidative reactions described above. The resulting ^{13}C isotope isomers, or isotopomers, can be detected by high-resolution ^{13}C NMR or mass spectrometry approaches (38, 39, 64, 65). The complexity of the model required to fit these isotopomers to fluxes depends on how many carbon transitions involve ^{13}C (34). For example, liver has a rate of anaplerosis from pyruvate that exceeds the rate of pyruvate dehydrogenase (PDH) activity by more than 10-fold. Thus, the model is simplified by ignoring the entry of ^{13}C-acetyl-CoA into the TCA cycle (14, 64). The anaplerotic metabolism of a [U-^{13}C]pyruvate tracer introduces contiguous ^{13}C labeling in C1, C2, and C3 (or C4, C3, and C2) of OAA, but not acetyl-CoA carbons, which become C3 and C4 (or C1 and C2) during oxidative turnover (**Figure 2*c***). Thus, acetyl-CoA dilutes the labeling of anaplerotic tracers as a function of the rates of anaplerosis and TCA cycle turnover (**Figure 2*d***), allowing these fluxes to be determined if the isotopomer distributions are known (14, 64) (**Figure 2*e***). Alternatively, a tracer that enters the TCA cycle as acetyl-CoA, but not anaplerosis, also provides isotopomers that indicate rates of anaplerosis. For example, [U-^{13}C]fatty acids are avidly metabolized to [U-^{13}C]acetyl-CoA in liver but cannot be used as an anaplerotic substrate in vertebrate animals. Thus, αKG (or glutamate) C4 and C5 will be labeled on every turn of the cycle, with C1, C2, and C3 becoming labeled on subsequent turns. Unlabeled anaplerotic substrate will dilute C1, C2 and C3, but never C4 and C5. Thus, dilution of ^{13}C isotopomers in the glutamate C2 and C3, relative to C4 and C5, indicates the relative rates of anaplerosis and TCA cycle turnover (11, 14, 142). Rates of anaplerosis in excess of TCA cycle turnover in human liver were detected by ^{13}C magnetic resonance spectroscopy (MRS) of hepatic glutamate C1 and C5, following [U-^{13}C]acetate infusion (11). In tissues like skeletal muscle, heart, β-cells, and brain, [U-^{13}C]pyruvate may be metabolized by both PDH- and pyruvate carboxylase (PC)-mediated anaplerosis, thus invalidating these simplified assumptions about ^{13}C transitions. The simultaneous oxidation and anaplerosis of pyruvate can be quantified by analysis of glutamate isotopomers in C1–C3, which informs anaplerosis, and in C4 and C5, which informs oxidation, but require a more detailed positional isotopomer analysis (125).

2.3. Label Recycling

Cataplerotic pathways that lead back to anaplerosis are common in metabolism and are accompanied by additional carbon transitions. This phenomenon, termed pyruvate cycling, was described by Friedman and colleagues (48), who unexpectedly detected the label from a [2-^{14}C]pyruvate tracer in positions C1 and C3 of pyruvate in liver. Pyruvate cycling occurred when carboxylation and symmetrization caused 50% of C2 OAA originating from pyruvate to be converted to C3 pyruvate upon cataplerosis. C1 labeling was generated by cataplerosis, following one turn of the TCA cycle (**Figure 3*a***). Thus, these isotopomers capture relative rates of anaplerosis, TCA cycle

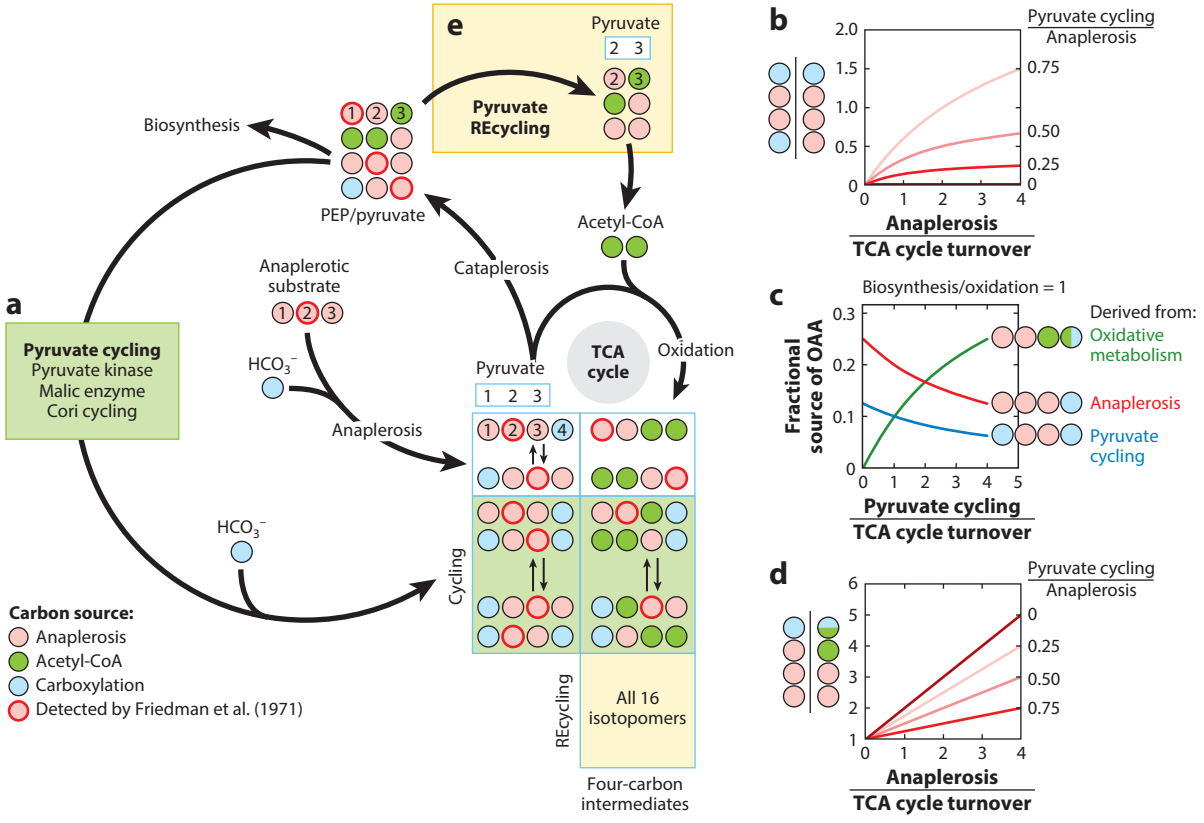

Figure 3

(*a*) Schematic illustrating the carbon transitions during pyruvate cycling. Pyruvate cycling was detected by Friedman et al. (48) when labeled C2 of an anaplerotic substrate (*red circles with red border*) underwent carboxylation and symmetrization that caused 50% of C2 OAA originating from pyruvate to be converted to C3 pyruvate upon cataplerosis. C1 labeling was generated by cataplerosis following one turn of the TCA cycle. (*b*) Pyruvate cycling generates OAA isotopomers enriched with carbons from carboxylation and depleted of carbons from the original anaplerotic substrate. The ratio of pyruvate cycling–derived OAA to anaplerosis-derived OAA increases as a function of both relative anaplerotic flux and relative pyruvate cycling. Note that the nonlinear relationships necessitate special consideration when examining isotope enrichments in tissues where anaplerosis is active. (*c*) Fractions of OAA derived from anaplerosis (*red line*), pyruvate cycling (*blue line*), and oxidative metabolism (*green line*) as a function of pyruvate cycling relative to TCA cycle turnover (example shown when the rates of biosynthesis and TCA cycle flux are equal). (*d*) The ratio of anaplerosis-derived OAA isotopomers to oxidation-derived OAA isotopomers increases linearly as a function of relative anaplerotic flux (as in **Figure 2*e***), but pyruvate cycling decreases the slope of this relationship (i.e., predictably lowers the ratio of isotopomers). (*e*) Pyruvate REcycling generates new acetyl-CoA isotopomers, which compounds the complexity of the isotopomer patterns and generates all 16 possible OAA isotopomers. Abbreviations: OAA, oxaloacetate; PEP, phosphoenolpyruvate; TCA, tricarboxylic acid.

turnover, cataplerosis lost to pyruvate cycling, and net cataplerosis for biosynthesis. A similar approach using [U-^{13}C]lactate or [U-^{13}C]propionate provides an analytical advantage for detecting these transitions, since contiguous ^{13}C labeling in OAA C1–C3 is easily distinguished from OAA isotopomers in which C1 is lost to pyruvate cycling. As the fraction of cataplerosis that undergoes pyruvate cycling increases, C1–C3 labeling is progressively converted to C2–C3 labeling (**Figure 3*b***). This process also increasingly dilutes anaplerotic carbons with acetyl-CoA, as pyruvate cycling decreases these carbons' probability of escaping to biosynthesis (**Figure 3*c***). Thus, the ratio of labeling in C1–C3 compared to C1–C2 is predictably lowered by the increasing contribution of pyruvate cycling to anaplerosis (**Figure 3*d***). Despite not contributing to net cataplerotic biosynthesis, cycling pathways alter carbon transitions of the TCA cycle.

Pyruvate cycling has been attributed to the decarboxylation activities of pyruvate kinase (PEP → Pyr) and/or malic enzyme (ME) (Mal → Pyr). Pyruvate cycling by the pyruvate kinase pathway may occur in gluconeogenic tissue to provide added metabolic control through futile cycling (52) or in separate tissue compartments during Cori cycling (55). The ME pathway may be used to recycle OAA following citrate lyase during lipogenesis. However, the actual nature of pyruvate cycling detected by an anaplerotic tracer is often ambiguous, and it is more commonly used as a modeling allowance than as a focus of biological significance (86). Pyruvate kinase, ME, Cori cycling, and exchange in a variety of carboxylation reactions all remove C1 of OAA, thereby generating indistinguishable carbon transitions. The observation of these carbon transitions is also tracer dependent. Lactate tracers that undergo anaplerosis to OAA but do not complete backward scrambling underestimate cycling compared with anaplerotic tracers that are symmetrized by virtue of entering the cycle as succinate (e.g., propionate) (55, 122). Nevertheless, both tracers give similar rates of net biosynthetic cataplerosis, despite ongoing debate about the nature of pyruvate cycling (55). A variant of pyruvate cycling, called pyruvate REcycling, occurs in tissues with active anaplerotic and PDH pathways. Rather than reentering the TCA cycle as OAA, pyruvate originating from cataplerosis is converted to acetyl-CoA and oxidized in the TCA cycle. Pyruvate REcycling allows anaplerotic nutrients to be oxidized. For example, this pathway is necessary for glutamine, propionate, and branched-chain amino acid (BCAA) oxidation. In a tracer experiment with ^{13}C anaplerotic substrates, pyruvate REcycling can generate all 4 ^{13}C-acetyl-CoA isotopomers, all 16 isotopomers of OAA, and 32 isotopomers of αKG (**Figure 3*e***); therefore, it requires more complex computational models to solve (125).

3. PATHWAYS OF CATAPLEROSIS AND ANAPLEROSIS IN BIOSYNTHESIS

> . . .and by putting [the old planks] afterwards together in the same order, had again made a ship of them, this, without doubt, had also been the same numerical ship with that which was at the beginning; and so there would have been two ships numerically the same, which is absurd.
>
> —Thomas Hobbes on Theseus's Paradox

3.1. Hepatic Gluconeogenesis

Phosphenolpyruvate carboxykinase (PEPCK) catalyzes the GTP-dependent decarboxylation of OAA to PEP. The most conspicuous role of PEPCK is to provide PEP to the gluconeogenic pathways in liver and kidney, but it also functions in nongluconeogenic contexts (25). There are two isoforms of PEPCK, one situated in the cytosol (*Pck1*; PEPCK-C) and one in the mitochondria

(*Pck2*; PEPCK-M), whose relative amounts are species and tissue dependent (10). Mouse liver expresses 95% *Pck1*; therefore, its regulation has been the most widely studied (25). Hepatic *Pck1* mRNA is upregulated 100-fold by fasting and is suppressed by feeding through hormone-mediated transcriptional regulation (25). PEPCK-C has a short half-life, which is regulated by acetylation events that promote its degradation (63). The activity of PEPCK-C is generally considered to be governed by protein concentration (25), but recent studies suggest that its activity can be reversed in the hyperacetylated state (80). The regulation of PEPCK-M is thought to be less dependent on hormone signaling than PEPCK-C (25). Human liver expresses roughly 50% of each isoform, and certain avian species express mainly PEPCK-M (25), suggesting that it must play a significant role in certain contexts (10). PEPCK-C is important when an oxidized cytosolic redox induces the transport of malate from mitochondria to cytosol. The oxidation of malate by cytosolic malate dehydrogenase produces NADH for redox control and OAA for PEPCK-C-mediated cataplerosis. When cytosolic redox state is reduced, malate export is inhibited, and PEP produced by PEPCK-M can be transported to the cytosol without affecting redox. The prominent expression of PEPCK-M in nongluconeogenic tissues, such as β-cells (61), brain (4), and certain cancers (95), allows anaplerotic substrates to enter the glycolytic pathway without losing NADH to the cytosol. However, genetic studies in mice indicate a more complex synergy between PEPCK isoforms. Although *Pck2* constitutes less than 10% of total hepatic PEPCK, knockdown of *Pck2* in rodent liver resulted in suppressed gluconeogenesis from lactate (127). Likewise, overexpression of *Pck2* augmented gluconeogenesis in wild-type mice but, surprisingly, was unable to rescue gluconeogenesis in liver-specific *Pck1* knockout mice (94), indicating that both isoforms are necessary. Indeed, human inborn errors of both *Pck1* and *Pck2* genes cause severe phenotypes, including hypoglycemia and liver failure (30, 138). Thus, cataplerosis by the two isoforms may have cooperative roles, with PEPCK-M being necessary but not sufficient for normal gluconeogenesis, though nevertheless more prominent in nongluconeogenic tissues of mice.

Mitochondria of liver have the highest cataplerotic flux of all major tissues, and most of this flux originates from PEPCK for carbohydrate synthesis. In humans, more than 1.5 OAAs are lost to cataplerotic gluconeogenesis for every OAA converted to citrate in the TCA cycle (17, 65, 86, 130). This pathway produces ~40% of circulating glucose after an overnight fast and up to 80% after glycogen depletion following 2 days of fasting (16). Thus, a 75-kg human produces 10 g of glucose per hour, 5 g of which originate from the TCA cycle of liver mitochondria. Despite the remarkable suppression of PEPCK-C by feeding (25), tracer studies demonstrated that flux through this pathway remains active, ostensibly to facilitate Cori cycling (93) and the indirect synthesis of glycogen (97). Indeed, insulin infusion in the canine model suppressed *Pck1* expression by 90% and PEPCK-C protein by 50%, but not cataplerotic flux to gluco/glyconeogenesis (41, 116). The continuation of hepatic cataplerosis despite downregulation of *Pck1* expression indicates that PEPCK-C is a weak regulator of flux. A sevenfold overexpression of PEPCK-C increased flux by only twofold (136). Likewise, a 70% and 90% loss of PEPCK-C protein caused a decline in flux by only 25% and 40%, respectively (20). While surprising in the context of transcriptional regulation, these functional data are consistent with metabolic control analyses in liver indicating that PEPCK-C concentration controls only 20% of its own flux (20, 52). Nevertheless, despite its modest control over cataplerotic flux, PEPCK-C function can inversely alter TCA cycle intermediate concentrations (122), which play important roles in signaling and redox (74, 88, 120).

Remarkably, a metabolic control analysis indicated that hepatic cataplerosis is controlled predominantly by PC-mediated anaplerosis (52). PC is located in mitochondria and catalyzes the ATP-dependent carboxylation of pyruvate to OAA. This reaction is necessary for the anaplerosis of lactate, alanine, and a variety of other amino acid sources of pyruvate. PC is expressed in

most tissues and is considered the anaplerotic counterpart of PEPCK-mediated gluconeogenesis in liver (22). However, in contrast to the exquisite transcriptional regulation of PEPCK, PC is controlled through allosteric regulation (1). PC is a tetrameric mitochondrial enzyme with separate regions containing an ATP-dependent biotin site for bicarbonate activation and a pyruvate binding transferase site. An allosteric site that binds acetyl-CoA induces a conformational change that brings these two regions into proximity and catalyzes pyruvate carboxylation (1). PC activity requires acetyl-CoA and has a binding constant in the physiological range of acetyl-CoA concentration, but it is also inhibited by ADP and αKG (90, 135, 140). The allosteric regulation of PC allows hepatic anaplerosis to be stimulated by fatty acid oxidation, which provides more than 90% of liver acetyl-CoA and increases ATP/ADP. This aspect of regulation may be why mouse models and humans with defects in fat oxidation have impaired gluconeogenesis and are vulnerable to hypoglycemia (21, 126). In contrast, increasing free fatty acid (FFA) delivery to liver increases gluconeogenesis within minutes, consistent with allosteric activation of PC and induction of energy production by fatty acid oxidation (146). The induction of gluconeogenesis by fatty acids is replicated in humans when circulating FFAs are supplemented by lipid infusion (119), and it is countered by suppressing adipose lipolysis (26). The ability of adipose lipolysis to influence hepatic anaplerosis is a remarkable example of interorgan communication, and it allows insulin and glucagon to regulate gluconeogenesis by directly acting on liver and indirectly acting on adipose lipolysis (118). Additional molecular studies identified similar mechanisms that mediate hormone-regulated lipolysis of intrahepatic triglyceride and fatty acid oxidation (150). Thus, despite not being an anaplerotic substrate, fatty acid oxidation elegantly links control of anaplerotic flux and energy availability for gluconeogenesis (**Figure 4**).

3.1.1. Hepatic anaplerosis and cataplerosis are stimulated by obesity and insulin resistance. During obesity (29), type 2 diabetes (T2DM) (32), and nonalcoholic fatty liver disease (NAFLD) (45), insulin fails to suppress cataplerotic PEPCK flux to gluconeogenesis. However, PEPCK-C is not overexpressed in all rodent models of diet-induced obesity or in humans with T2DM (121). In fact, normalization of gluconeogenic flux in a high-fat diet–fed mouse model requires that PEPCK-C be reduced by 70% below normal (122), and a 50% knockdown was insufficient to normalize plasma glucose in a genetic mouse model of T2DM (51). These surprising findings may be related to the stimulation of anaplerosis, rather than the direct activation of cataplerosis during diabetes. Indeed, loss of insulin action triggers events that facilitate the energetic requirements and allosteric activation of both gluconeogenesis and anaplerosis. Adipocyte insulin resistance causes increased lipolysis and FFA delivery to liver (12), elevated fat oxidation, and allosteric activation of PC-mediated anaplerosis, analogous to the effect of exogenous FFAs (119, 146). Loss of hepatic insulin action independently increases fat oxidation, thus supplying ample ATP to drive the endergonic reactions of gluconeogenesis (75). Remarkably, glycemic regulation is normal in the absence of hepatic insulin action if the transcription factor FOXO1 is also removed to prevent overexpression of gluconeogenic and oxidative programs (133). Glycemia and gluconeogenesis became elevated only when oxidative metabolism and acetyl-CoA levels were increased by infusion of an exogenous oxidative substrate, consistent with a prominent role of adipose insulin resistance in fueling excess gluconeogenesis (111). Insulin resistance also increases Cori cycling and proteolysis in muscle, which contribute lactate and alanine as anaplerotic substrates that supply gluconeogenesis in T2DM and obesity (29, 32). In addition, glycerol generated during lipolysis was found to be largely converted to circulating lactate (124, 143), which may explain why glycerol as a direct precursor for gluconeogenesis is not affected as strongly as gluconeogenesis from anaplerotic substrates in insulin-resistant humans (29). Thus, insulin resistance and obesity may overactivate anaplerosis and gluconeogenesis by promoting substrate-replete conditions in liver.

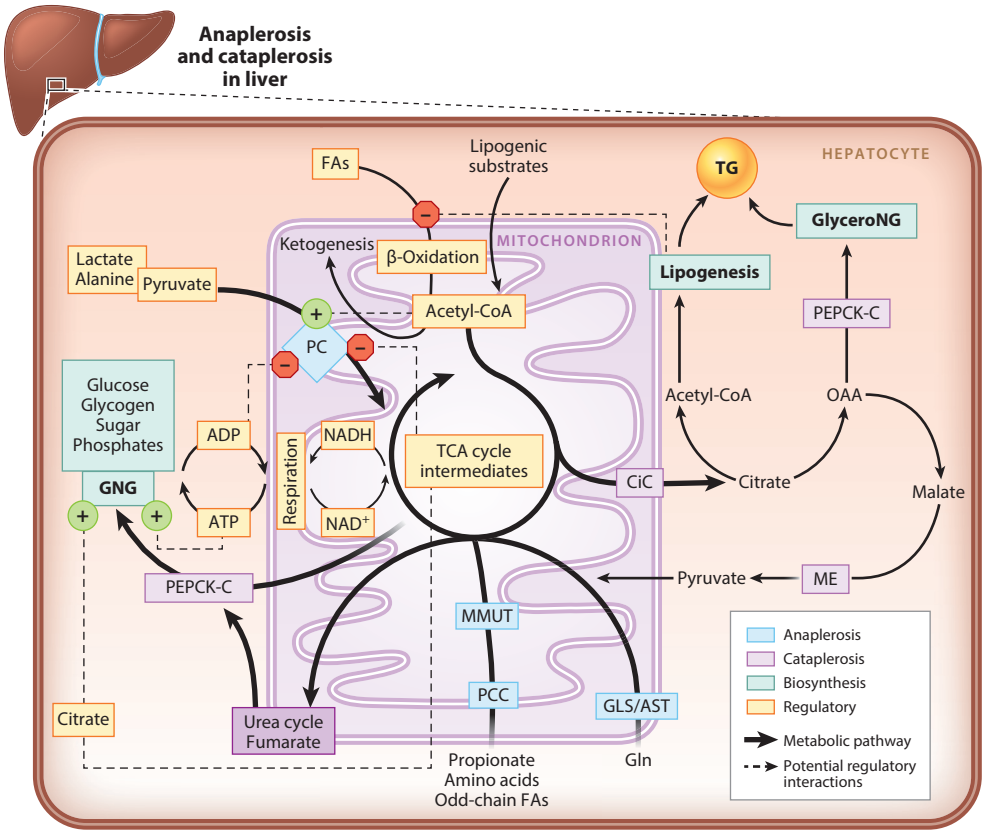

Figure 4

Pathways of anaplerosis and cataplerosis that play critical roles in liver GNG, GlycoNG, GlyceroNG, lipogenesis, and urea production. PC carboxylates pyruvate to OAA and is a key pathway in the control of GNG. PC is allosterically activated by acetyl-CoA and is inhibited by ADP and αKG. PEPCK is a cataplerotic pathway that catalyzes the decarboxylation of OAA to phosphoenolpyruvate and plays roles in GNG, GlyceroNG, and glycogen synthesis. Fumarate formed in the urea cycle can be converted to cytosolic OAA and used in the PEPCK pathway. ME heavily favors the cataplerotic decarboxylation of malate to pyruvate and participates in lipogenesis. PCC and MMUT are essential for the anaplerosis of BCKAs derived from systemic BCAAs and odd-chain FAs. Anaplerosis through αKG begins with glutamine, as illustrated in **Figure 5**. Abbreviations: BCAAs, branched-chain amino acids; BCKAs, branched-chain ketoacids; CiC, citrate-isocitrate carrier; FA, fatty acid; GLS/AST, glutaminase/aspartate aminotransferase; GlyceroNG, glyceroneogenesis; GlycoNG, glyconeogenesis; GNG, gluconeogenesis; ME, malic enzyme; MMUT, methylmalonyl-CoA mutase; OAA, oxaloacetate; PC, pyruvate carboxylase; PCC, propionyl-CoA carboxylase; PEPCK, phosphoenolpyruvate carboxykinase; TCA, tricarboxylic acid; TG, triglyceride; αKG, α-ketoglutarate.

3.1.2. Hepatic anaplerosis and TCA cycle metabolism during nonalcoholic fatty liver disease. Overactivation of anaplerosis may also be involved in the dysregulation of hepatocellular energetics in animal models and humans with NAFLD (42, 45, 69, 122, 130). Overnight-fasted obese humans with NAFLD have elevated lipolysis and the expected induction of anaplerosis and gluconeogenesis, and they also have elevated oxidative TCA cycle turnover (130). Surprisingly, prolonged fasting in a similar cohort of subjects produced markedly lower circulating FFAs, ostensibly due to lingering hyperinsulinemia, yet the subjects retained slightly higher rates of gluconeogenesis from anaplerosis (45). Notably, these individuals had modestly impaired ketogenesis and elevated TCA cycle flux, indicating that acetyl-CoA was preferentially oxidized in

lieu of normal activation of fasting ketogenesis. The cause of this altered acetyl-CoA partitioning in NAFLD during fasting is unclear, but elevated anaplerosis may provide increased OAA, a factor which is known to favor acetyl-CoA metabolism in the TCA cycle over ketogenesis. Likewise, when ketogenesis was genetically inhibited in mice, TCA cycle metabolism and gluconeogenesis were stimulated, and hepatocellular damage was worsened (33, 35). Forcing acetyl-CoA into the TCA cycle increases the respiratory load compared with ketogenesis and may create more oxidative stress (27), especially as NAFLD progresses to impaired respiratory capacity during nonalcoholic steatohepatitis (NASH) (69). Low-carbohydrate diets divert acetyl-CoA to ketones and require high rates of β-oxidation to maintain energy status, thereby rapidly lowering steatosis, but do not induce anaplerosis or oxidative TCA cycle metabolism (17, 85). Hepatic mitochondrial pyruvate carrier inhibition in animal models restricts anaplerosis (91), prevents the overactivation of TCA cycle metabolism (117), and protects against the development of NASH (92). Conversely, pharmacological respiratory uncouplers reduce steatosis by accelerating acetyl-CoA oxidation in the TCA cycle and suppress anaplerosis, likely due to lower acetyl-CoA and/or depressed energy status (50). Interventions that induce gluconeogenesis and TCA cycle metabolism can also have protective effects in liver. Acute exercise markedly elevates flux through these pathways to support peripheral glucose utilization (57) and chronic exercise protects against NAFLD by increasing fat oxidation (132). Sodium glucose cotransporter 2 (SGLT2) inhibitors increase glucose disposal by glucosuria, and they may have similar effects as exercise by activating compensatory gluconeogenesis and ketogenesis (43). It is notable that increasing gluconeogenic demand, limiting oxidative substrate, reducing oxidative efficiency, and treating with pharmacological uncouplers may have the common effect of lowering mitochondrial membrane potential and decreasing oxidative stress during nutrient excess (27).

3.2. Extrahepatic Gluconeogenesis

The only quantitatively significant source of extrahepatic gluconeogenesis occurs in the kidney (115). PEPCK-C is highly expressed in the proximal tubules of the renal cortex, where it facilitates cataplerosis following anaplerosis of glutamine carbons. The resulting ammonia neutralizes metabolic acidosis and is secreted into urine, and the anaplerotic αKG undergoes cataplerotic gluconeogenesis. This pathway is considered a negligible source of circulating glucose under most conditions but may rise to more than 25% during metabolic acidosis, starvation, and type 1 diabetes (129). Compensation by renal gluconeogenesis can support normal fasting glycemia in mice with liver-specific loss of gluconeogenic function (22) and is markedly induced in humans during the anhepatic phase of liver transplantation (9). The mechanism for this compensatory activation of renal gluconeogenesis is unclear. While hepatic *Pck1* is regulated by glucagon and insulin, renal *Pck1* is thought to be upregulated by glucocorticoids and metabolic acidosis (25). In contrast to PC regulation of anaplerosis in liver, anaplerosis in the renal cortex is induced by increased glutamine delivery from peripheral tissues and activation of glutaminase (GLS) and glutamate dehydrogenase (GDH) by acidosis (25). More recently, it was reported that insulin resistance and hypoxia-inducible factor 1α signaling induce proximal tubule *Pck1* expression, suggesting the potential for enhanced renal gluconeogenesis during obesity and diabetes (105). SGLT2 inhibition, which prevents the reabsorption of glucose in the proximal tubule and improves insulin resistance, induced PEPCK levels and renal gluconeogenesis in some mouse studies (62) but suppressed it in others (131). Likewise, one study associated the activation of gluconeogenesis with diabetic nephropathy (62), while another found that the inhibition of gluconeogenesis protected against nephropathy (131). In the latter case, differential effects on cataplerosis and anaplerosis by SGLT2 inhibition lowered TCA cycle intermediates in the renal cortex and prevented oxidative stress (131).

Understanding renal anaplerosis and cataplerosis may provide valuable insight into kidney disease beyond its contribution to endogenous glucose production.

PEPCK-C is also expressed in the enterocytes of the small intestine, where it has been proposed to support a small amount of glucose release (139). This rate cannot be measured in vivo (115), and ex vivo experiments indicate that it is too low to directly affect endogenous glucose production (113). Enterocyte-specific PEPCK knockout mice had normal glycemic regulation in the fed, fasted, and diabetic states but had abnormal amino acid profiles and slower intestinal lipid absorption, highlighting the importance of intestinal cataplerosis in amino acid processing and glyceroneogenesis (113). However, intestinal gluconeogenesis might play an indirect role in glycemic regulation through gut–brain signaling by producing small amounts of glucose detected by afferent nerves of the portal system (139). Glucose 6-phosphatase knockout mice were reported to lose some of the beneficial effects provided by intragastric organic acid administration and were more susceptible to liver steatosis on a carbohydrate diet (139). The mechanisms involved in this process remain to be determined.

3.3. Lipogenic Tissue

Lipogenesis occurs in most tissues for the maintenance of organelle membranes and growth, but it is most active in liver and adipose during feeding to convert excess carbohydrate to lipid for long-term calorie storage (141). Lipogenesis occurs in the cytosol through the condensation of consecutive units of acetyl-CoA, most of which is derived from mitochondrial PDH during carbohydrate metabolism. For mitochondrial acetyl-CoA to be trafficked to the cytosol, it is first condensed with OAA to generate citrate in the first step of the TCA cycle, and it is then actively transported by the citrate-isocitrate carrier (CiC) (112). Cytosolic ATP–citrate lyase regenerates OAA and acetyl-CoA in the cytosol. These steps remove citrate from mitochondria and therefore require continuous anaplerosis to maintain lipogenesis (106). Interestingly, in vitro characterization of the CiC indicates that it couples citrate transport with malate antiport (109). Thus, cytosolic OAA could be converted to malate and exchanged back into the mitochondria with no further carbon transitions, obviating the need for other anaplerotic support. However, loss of CiC causes decreased TCA cycle pool size and lactate accumulation in cell models and humans (109), suggesting that citrate transport is critical to anaplerotic and cataplerotic homeostasis. Indeed, NAFLD subjects have elevated lipogenesis (78), coincident with increased hepatic anaplerosis and citrate synthase flux (130). Tracer studies indicate that citrate lyase is a significant source of OAA used by PEPCK-C (39). This pathway contributes to glycerol-3-phosphate for fatty acid esterification via the glycerol-3-phosphate acyltransferase pathway and is particularly important in adipose tissue, which lacks glycerol kinase (106). When this pathway is removed from adipocytes by PEPCK-C deletion, mice become lipodystrophic upon carbohydrate restriction (25). In liver, the majority of the OAA returns to the TCA cycle following ME conversion of malate to pyruvate and subsequent anaplerosis by pyruvate carboxylation, which has the metabolic advantage of providing NADPH required in the lipogenic pathway (39). Knockdown of liver and adipose PC in rats suppresses lipid synthesis by decreasing glyceroneogenesis (76), and liver-specific PC knockout mice have decreased circulating triglycerides (22). It remains unclear whether insulin-resistant dysregulation of cataplerotic gluconeogenesis and lipid synthesis share common metabolic mechanisms.

3.4. Central Nervous System

PC is the most abundant anaplerotic enzyme in brain and is largely expressed in astrocytes (123). Rare PC loss-of-function mutations in humans cause severe metabolic and neurological impairments (87). Notable defects in glucose, amino acid, and urea cycle function suggest a

primary liver phenotype with neurotoxic effects (87). However, anaplerotic therapies and liver transplant led to only moderate improvements in neurological symptoms (87), and liver-specific PC knockout mice had no neurological or motor phenotype (22). Astrocytic anaplerosis via PC allows αKG cataplerosis for glutamate and glutamine (Glx) synthesis during glutaminergic neurotransmission (123). Tracer studies indicate that PC flux is roughly 30% of the Glx cycle, suggesting that PC flux is critical for maintaining this pool (107). The regulation of astrocyte PC by acetyl-CoA is thought to be retained, but the rationale for this regulation is less clear compared with liver, where the rate of acetyl-CoA generation by fat oxidation has an extraordinary physiological range. However, ATP utilization for neurotransmission is high in astrocytes, suggesting a metabolic benefit for positive regulation of neurotransmitter synthesis by cellular energetics. For example, neuroglial pyruvate carboxylation was increased by brain activity (107), and inhibition of anaplerosis suppressed both TCA cycle flux and oxygen utilization during whisker stimulation in rodents (89).

PC is also active in oligodendrocytes, where it is proposed to support lipid synthesis for synaptic and myelin membranes, a process that depends on citrate transport from mitochondria and pyruvate cycling via ME, as described above (6). In fact, pyruvate cycling occurs extensively in brain to recycle neurotransmitters synthesized from anaplerosis (123). The activity of this pathway correlates strongly with ME levels (24), but the fate and compartmental location of recycled pyruvate remain a matter of discussion. Evidence for the activity of pyruvate REcycling was provided by the observation of [1-^{13}C]acetyl-CoA formation following [2-^{13}C]acetate administration (24), which occurs as shown in **Figure 3**. ^{13}C MRS studies indicated separate TCA cycle compartments, consistent with anaplerosis in glia and REcycling in neurons (24). Other studies demonstrated that pyruvate cycling occurs in both astrocytes and neurons, and that it might be more quantitatively significant as a mechanism to efflux cataplerotic carbons from the brain as lactate (123). Whatever the case, operation of the ME pathway is notable for its role in maintaining NADPH redox, which is likely to be physiologically significant in antioxidant mechanisms. Notably, anaplerotic flux is altered in several animal models of neurological disease, including ischemic brain injury (98), Alzheimer's disease (145), and seizure disorders, some of which respond favorably to anaplerotic therapies like triheptanoin (144, 149).

3.5. Porphyrin Synthesis

In contrast to the cataplerosis of OAA via PEPCK, which is relevant to multiple pathways, the cataplerosis of succinyl-CoA is specific to the synthesis of porphyrins and hemoproteins. The enzyme δ-aminolevulinic acid synthase (ALAS) condenses succinyl-CoA and glycine to δ-aminolevulinic acid in the mitochondria as the first step of heme synthesis. The molecular and metabolic regulation of this step and related pathways have been thoroughly reviewed elsewhere (110). ALAS1 is ubiquitously expressed and is necessary to maintain homeostasis of mitochondrial and cytosolic hemoproteins involved in oxygen transport, oxygen binding, and electron transport. Because of their reactive environment, these proteins have short half-lives and are produced on demand (147). ALAS1 is activated by highly oxidative conditions, such as increased respiration or Cyp450-mediated catabolism of xenobiotics, and it is suppressed by elevated heme content through feedback inhibition (2). There are no known inborn errors of ALAS, but defects in the heme pathway cause ALAS to remain activated, leading to porphyrias (110). Despite operating at a fraction of PEPCK flux, ALAS overactivation suppresses TCA cycle function by depletion of succinyl-CoA and inhibition of complex 2 (56).

ALAS2 is expressed exclusively in erythroblasts of bone marrow and erythroid committed precursors. It is upregulated in response to free iron and functions to fulfill hemoglobin requirements during erythrocyte development (110). This cataplerotic pathway persists only until the mitochondria are lost during the late stages of red blood cell maturation. ALAS2 function was found to be

exclusively reliant on glutamine-derived αKG, but tracer studies indicated that this αKG does not equilibrate with other TCA cycle intermediates (18). Thus, ALAS2 is a unique example of a pathway that uses a TCA cycle intermediate for biosynthesis without technically being cataplerotic.

4. CATABOLIC FUNCTIONS OF ANAPLEROSIS AND CATAPLEROSIS

> One cannot step twice into the same river. . . it scatters and again gathers; it forms and dissolves, and approaches and departs.
>
> —Heraclitus

4.1. Anaplerotic Substrate REcycling

REcycling is required for an anaplerotic substrate to be oxidized in the TCA cycle. For example, to oxidize the five carbons of glutamine, it must enter the TCA cycle as αKG, undergo one decarboxylation in the TCA cycle to malate/OAA, one decarboxylation by ME to generate pyruvate, one decarboxylation by PDH to generate acetyl-CoA, and finally two decarboxylations in one turn of the TCA cycle. The combined reactions of the ME and PDH constitute pyruvate REcycling in this example and are required to maintain mass balance of the TCA cycle during glutamine oxidation. The ME catalyzes the following equilibrium reaction: $Mal + NADP^+ \rightleftharpoons Pyr + CO_2 + NADPH$. Under most conditions, the equilibrium heavily favors the cataplerotic decarboxylation of malate to pyruvate (137). Unlike PEPCK, ME is ubiquitously expressed (40), but it does not directly facilitate biosynthesis, because pyruvate, unlike PEP, cannot directly enter the triose pool. The major role of ME is to recycle malate during lipid synthesis, and it is the most common pathway involved in anaplerotic substrate REcycling. This pathway also provides cytosolic NADPH for lipid synthesis, antioxidant function, and cell signaling in some tissues.

4.2. Nitrogen Trafficking

The ability to catabolize and resynthesize proteins, oxidize amino acids, or use their carbons in anaplerotic and biosynthetic pathways depends on managing the fate of nitrogen. Free ammonia is cytotoxic; therefore, mammalian biology has developed mechanisms to transfer nitrogen between metabolites in peripheral tissues, blood, and finally liver, where it can be safely sequestered as urea before renal secretion. In between, there are transaminase reactions, amino acids, and organic acids that act as an elegant bucket brigade to safely traffic nitrogen between tissues and scavenge free ammonia. Anaplerotic and cataplerotic pathways of peripheral tissue and liver are essential to this process.

4.2.1. Skeletal muscle. Skeletal muscle supports high rates of anaplerosis during exercise, but the mechanism and purpose of this pathway are poorly understood (49). Electrically stimulated contraction of soleus muscle increased anaplerosis to 20–40% of total TCA cycle flux, and remained at this proportion throughout contraction, implying that absolute rates of anaplerosis could increase by 100-fold, similar to O_2 consumption, during exercise (142). Acute exercise increases the concentration of TCA cycle intermediates by approximately fivefold, perhaps to magnify the capacity of the TCA cycle during exercise, but this interpretation has been disputed (15). In fact, activation of cataplerosis by overexpression of PEPCK-C in skeletal muscle paradoxically increases exercise capacity by 20-fold (54), and obese mice with low exercise capacity have twofold-lower PEPCK-C activity in muscle (104). It was suggested (54) that PEPCK-C overexpression increases intracellular lipid reserves by activating glyceroneogenesis, but it is unknown whether elevated cataplerotic capacity alters pool sizes or whether a specific end

product is important in exercise capacity. More commonly, anaplerosis in muscle is thought to facilitate proteolysis, amino acid oxidation, and ammonia scavenging, especially during exercise (**Figure 5**). This process may be partially regulated by CLOCK genes, suggesting that optimal nitrogen trafficking, anaplerosis, and potentially exercise capacity are modified by circadian mechanisms (46). Acutely, a rapid rise in glycolysis during exercise provides surplus pyruvate for PC, ME, or the alanine aminotransferase (ALT) reaction. Some investigators have emphasized the ALT mechanism, since alanine synthesis from pyruvate allows the net export of a nitrogen as alanine and the anaplerosis of αKG (15). αKG can undergo REcycling by the ME pathway for complete oxidation or be exported as lactate, but in the presence of high pyruvate, the mass action of ME causes TCA cycle intermediates to accumulate. The release of free ammonia during proteolysis is mediated by the purine nucleotide cycle (PNC). This pathway consumes aspartate, generated by the combined reactions of branched-chain amino acid aminotransferase/aspartate aminotransferase (BCAAT/AST) or ALT/AST, and produces ammonia and fumarate by deamination, analogous to the urea cycle in liver (8). Fumarate generated in this process replaces the OAA consumed in the AST reaction, and the ammonia is scavenged by GS to glutamine and exported from muscle. The importance of this pathway as a contributor to muscle anaplerosis during exercise has been debated (15), but inborn errors in the PNC do produce moderate effects on skeletal muscle anaplerosis and exercise capacity (44). Both ALT and the PNC allow muscle to export nitrogen to liver by continuous anaplerotic and cataplerotic cycling of organic acids, but the ALT pathway requires a constant supply of pyruvate as an amino acceptor, while the PNC depends on a constant supply of glutamic acid as an ammonia acceptor (**Figure 5**).

The BCAAs isoleucine and valine undergo transamination (BCAAT) to branched-chain ketoacids (BCKAs), which are converted to succinyl-CoA by a series of reactions culminating in propionyl-CoA carboxylase and methylmalonyl-CoA mutase (MMUT). Methionine and threonine also produce succinyl-CoA through the MMUT pathway, while the aromatic groups of phenylalanine and tyrosine are converted directly to fumarate by fumarylacetoacetate hydratase. Oxidation of these amino acids requires both nitrogen trafficking pathways and REcycling pathways in the TCA cycle. BCAAT is expressed primarily in muscle, but BCKAs can escape into circulation and become anaplerotic substrates in a variety of tissues, including liver (102). The contribution of BCAA anaplerosis to nonprotein macronutrient synthesis (e.g., gluconeogenesis) is probably low on the basis of their 40-fold-lower turnover rates compared with lactate (58, 102). However, these pathways are essential for amino acid catabolism, and their loss of function causes lethal metabolic defects in humans (53). A more subtle loss of BCAA homeostasis occurs in obesity and contributes to metabolic dysfunction, perhaps by impinging on insulin secretion from β-cell and insulin action in peripheral tissues through activation of mechanistic target of rapamycin complex 1 signaling (101).

4.2.2. Urea cycle. Amino acids and ammonia released from peripheral tissue are sequestered by the urea cycle in liver. The urea cycle converts one free ammonia and one aspartate to one urea and one fumarate. The stoichiometry of this process dictates the roles of anaplerosis and cataplerosis in nitrogen disposal (**Figure 5**). In principle, the amino group of alanine could be trafficked to urea by the combined reactions of ALT, AST, and the urea cycle. The OAA lost to aspartate could be regenerated as fumarate by the urea cycle with no net loss of TCA cycle intermediates. However, this sequence is not self-sustaining for two reasons. First, PC knockout liver accumulates urea cycle intermediates and is depleted of aspartate, indicating that cataplerotic flux to gluconeogenesis outcompetes the AST reaction for OAA (22). Thus, anaplerotic flux

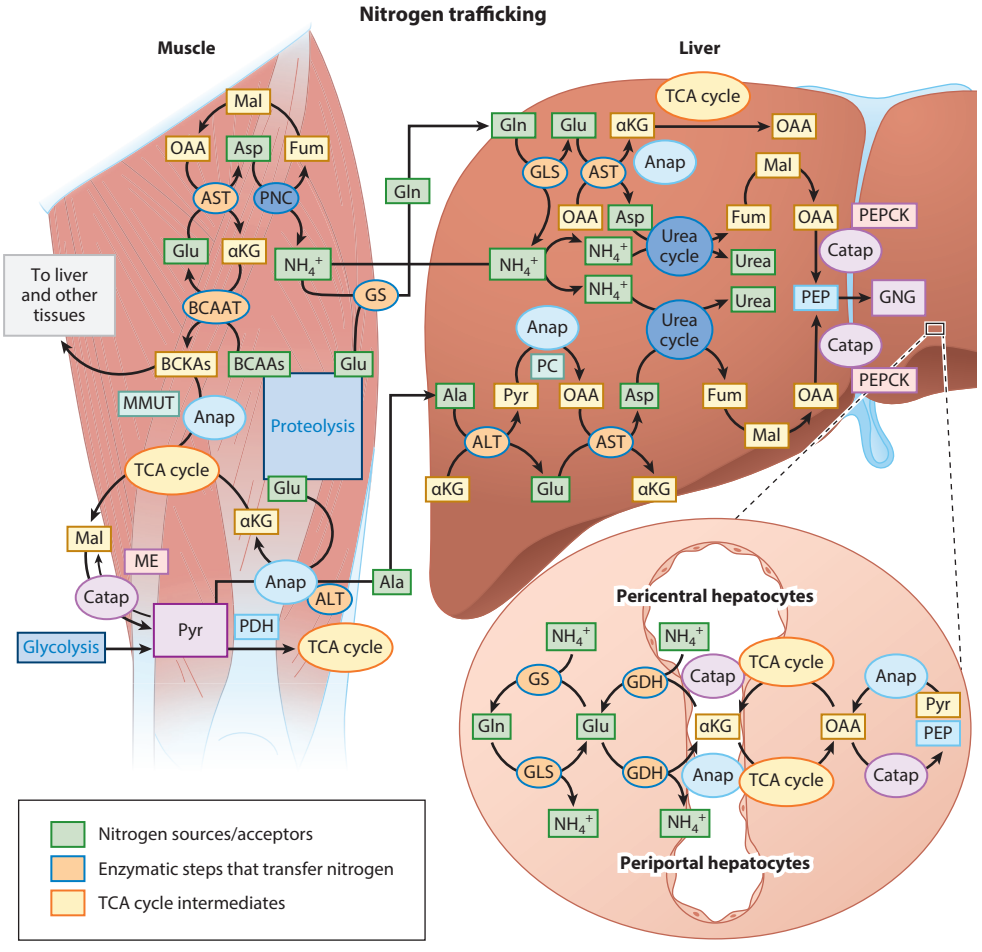

Figure 5

Nitrogen moieties from amino acids released by proteolysis are trafficked to alanine or glutamine in muscle. ALT transfers the amino group from glutamate to pyruvate with the anaplerosis of αKG. BCAAs transfer amino groups to glutamate and become anaplerotic substrates through the MMUT pathway. Anaplerotic carbons undergo pyruvate REcycling to be oxidized in the TCA cycle. Glutamate transfers amino groups to aspartate by the AST reaction and generates ammonia and fumarate by the PNC pathway. Ammonia and glutamine (following GS), are exported to liver. In liver, alanine transfers its amino group to urea by the combined reactions of ALT, AST and the urea cycle, but requires PC-mediated anaplerosis to maintain cataplerotic GNG from alanine and ammonia to complete the urea cycle. Catabolism of glutamine proceeds through the combined reactions of GLS, AST, and the urea cycle. GS and GDH function in pericentral hepatocytes to scavenge ammonia, while GLS and GDH function in periportal hepatocytes to generate ammonia for the urea cycle. Abbreviations: ALT, alanine aminotransferase; anap, anaplerosis; AST, aspartate aminotransferase; BCAAs, branched-chain amino acids; BCAAT, branched-chain amino acid transamination; BCKA, branched-chain ketoacid; catap, cataplerosis; GDH, glutamate dehydrogenase; GLS, glutaminase; GNG, gluconeogenesis; GS, glutamine synthetase; ME, malic enzyme; MMUT, methylmalonyl-CoA mutase; OAA, oxaloacetate; PC, pyruvate carboxylase; PDH, pyruvate dehydrogenase; PEP, phosphoenolpyruvate; PEPCK, phosphoenolpyruvate carboxykinase; PNC, purine nucleotide cycle; TCA, tricarboxylic acid; αKG, α-ketoglutarate.

through PC is required to replace the OAA consumed in the AST reaction (**Figure 5**). Second, the aspartate generated by this sequence cannot dispose of its amino group in the urea cycle in the absence of an independent source of ammonia. Likewise, glutamine anaplerosis through the combined GLS and GDH reactions results in two free ammonias and a stoichiometric mismatch of the urea cycle in the absence of an independent source of aspartate (**Figure 5**). These stoichiometric restrictions are generally met by a continuous supply of ammonia and amino acids from muscle. In addition, GDH may buffer urea cycle stoichiometry by acting in the anaplerotic direction during an ammonia deficit and in the cataplerotic direction during an ammonia surplus (**Figure 5**). Mice with liver-specific knockout of GDH developed hyperammonemia, lower liver aspartate, and decreased urea production (66). Remarkably, the glycemic response to a glutamine challenge was normal, but an alanine challenge produced a blunted response (66). Presumably, glutamine continued to be anaplerotic through the GLS/AST pathway, which produces stoichiometric amounts of ammonia and aspartate (**Figure 5**). However, aspartate generated by the ALT/AST pathway could not be used for gluconeogenesis in the absence of GDH to maintain the stoichiometry of the urea cycle. Importantly, GS is restricted to pericentral hepatocytes, allowing ammonia that escapes the urea cycle of periportal hepatocytes to be sequestered as glutamine, but this pathway also requires anaplerosis and cataplerosis to provide glutamate as the ammonia acceptor (13) (**Figure 5**).

4.3. Heart

Cardiac anaplerosis is less than 10% of total TCA cycle flux in the normal myocardium (49). This pathway plays a housekeeping role by maintaining TCA cycle intermediates that are lost to transamination reactions or excretion from the myocardium (49). Heart failure doubles the rate of anaplerosis for reasons that are unclear. The normal heart oxidizes very little glucose, but a shift to glycolysis during heart disease may stimulate anaplerosis by increasing myocardial pyruvate availability (49). Pharmacologic activation of PDH (114) or genetic activation of fat oxidation (70) reduced anaplerosis and improved contractile function, suggesting that elevated anaplerosis is maladaptive. In contrast, mitochondrial pyruvate carrier knockout mice, which cannot transport pyruvate into mitochondria, surprisingly maintained glucose oxidation and had only a modest reduction in anaplerosis, indicating alternative routes of anaplerosis and pyruvate trafficking into mitochondria (151). Other potential pathways have been noted. For example, reversal of the myocardial cytosolic ME1 supports the anaplerosis of malate from pyruvate in a rat model of hypertensive heart disease (77). Inhibition of ME1 by microRNA normalized anaplerotic flux and improved contractile function. An important difference between PC- and ME-mediated pyruvate carboxylation is that the latter consumes NADPH, a factor that contributes to impaired antioxidant response in heart failure (77). However, a mouse model of severe transverse aortic constriction induced anaplerosis through succinyl-CoA or αKG but not pyruvate carboxylation (134). Most tracer studies of anaplerosis in heart failure have relied on ex vivo animal models, but a recent human study used metabolomic arterial/venous differences to determine cardiac substrate metabolism in subjects with reduced ejection fraction (EF) (100). The normal human heart supplied more than 80% of its energy requirements from fatty acids, similar to rodent heart (70, 77, 114, 134, 151), but unlike in rodents, glucose utilization was not detected in human subjects with normal or reduced EF (100). However, the release of glutamine, alanine, and other amino acids was doubled in subjects with reduced EF. These data suggest that increased proteolysis in the myocardium may contribute to elevated anaplerosis and cataplerosis in heart disease (100).

4.4. Energetics and Redox

Anaplerosis and cataplerosis influence cellular energy status by mediating TCA cycle capacity, the equilibrium of redox reactions, and the supply of precursors to energetically costly biosynthetic pathways. In liver, gluconeogenesis from TCA cycle intermediates consumes roughly 40% of hepatic energy requirements (79, 122). Thus, there is a substantial decline in TCA cycle flux when hepatic anaplerosis is prevented by loss of PC, or when cataplerosis is prevented by loss of PEPCK-C (22, 122). In both cases, energy charge is elevated during fasting, suggesting that the reduction in TCA cycle flux is an adaptive response to decreased energy demand in the absence of gluconeogenesis.

In contrast, inhibition of anaplerosis has a dramatically different effect on redox metabolism than inhibition of cataplerosis. Loss of cataplerosis causes an accumulation of TCA cycle intermediates and a reduced redox state (low NAD^+/NADH) (19), while the loss of anaplerosis depletes TCA cycle intermediates and causes a more oxidized redox state (high NAD^+/NADH) (22). These effects on redox may be mediated by mass action through a network of equilibrium redox reactions (74). For example, loss of PC inhibits the urea cycle and causes an accumulation of ammonia, which shifts the GDH equilibrium (Glu + $NAD^+ \rightleftharpoons$ αKG + NH^4 + NADH) toward a more oxidized state. Similarly, loss of anaplerosis depletes malate and shifts the ME equilibrium (Mal + $NADP^+ \rightleftharpoons$ Pyr + NADPH) toward a more oxidized NADP(H) state, while loss of cataplerosis causes malate accumulation and a more reduced redox NADP(H) state. These effects are transmitted to the glutathione redox system, resulting in impaired reactive oxygen species (ROS) scavenging in the PC knockout liver and improved ROS scavenging in PEPCK knockdown mice, despite both having very similar glucose phenotypes. Notably, changes in TCA cycle intermediate concentrations also play a role in a variety of signaling pathways, including inflammation and oxidative stress (88, 120). Thus, small mismatches in the dynamic equilibrium of anaplerotic and cataplerotic function may alter pool sizes, without changing flux, and have yet-to-be-discovered effects on physiology and disease.

Pancreatic β-cells support a rate of anaplerosis that is nearly equal to the oxidative flux of the TCA cycle, and like liver, this pathway affects cellular energy status and physiological function. However, unlike liver, which releases cataplerotic products (i.e., glucose), the β-cell uses REcycling pathways to generate energetic and redox-linked signaling factors to sense nutrients and release insulin (60). When β-cells oxidize glucose, there is a rapid rise in ATP/ADP and Ca^{2+}, which stimulates an acute phase of insulin secretion. But, to sustain insulin secretion, β-cells require glucose carbons to undergo anaplerosis-mediated pyruvate REcycling (60). The mechanism by which substrate cycling helps sustain insulin release remains an active topic of research, but has thus far been attributed to the NADPH-linked reactions of ME and IDH1 (60), which promote glutathione (reduced form) formation and other signaling factors (59). Recently, cataplerosis by PEPCK-M was also described as a mediator of insulin secretion by altering mitochondrial GTP as a signaling factor (61). The field of β-cell research was among the first to recognize the importance of anaplerotic and cataplerotic pathways as signals for mediating cell function, a factor that is increasingly observed in many tissues and disease (88, 120).

5. ADAPTIVE ROLES OF ANAPLEROSIS AND CATAPLEROSIS IN CANCER

Cancer cells have a remarkable capacity to adapt anaplerotic, cataplerotic, and TCA cycle function to maintain growth, despite remarkable genetic and environmental handicaps. A well-established feature of many cancers is their unusual reliance on the anaplerosis of glutamine (37). Although glutamine has the metabolic advantage of being less susceptible to hypoxic tumor environments

compared with pyruvate, it is not an anaerobic-friendly substrate. Anaplerosis and cataplerosis of glutamine carbons to pyruvate produce four reducing equivalents, and a total of nine reducing equivalents when the resulting pyruvate is oxidized through the pyruvate REcycling pathway. Therefore, a distinctive characteristic of cancer metabolism is its ability to consume reducing equivalents by converting αKG to isocitrate through reverse IDH flux, or reductive carboxylation (37). Both hypoxia and impaired respiration in tumors provoke high NADH/NAD^+ and shift the equilibrium of IDH toward elevated isocitrate/αKG, while NADP(H)-dependent mitochondrial IDH1 and cytosolic IDH2 bypass the thermodynamic restrictions of the mitochondrial and NAD(H)-dependent IDH3 isoform (108). Citrate produced through this pathway is critical for lipid synthesis when the TCA cycle is inhibited due to hypoxia or impaired respiration (108). The role of IDH1/2 isoforms in cancer helped clarify the appearance of M+5 citrate isotopomers originating from M+5 [U-$^{13}C_5$]glutamine, which could otherwise be interpreted as exchange through reversible reactions (39). When flux was modeled in subcellular fractions of cancer cells, cytosolic reductive carboxylation was less than 15% of oxidative flux, but it contributed all of the acetyl-CoA for lipogenesis (82). The plasticity of anaplerotic pathways is especially pronounced in cancer cells with mutations in succinate dehydrogenase (SDH), fumarate hydratase, or OGDH (23, 36, 47, 99), which rely on reductive carboxylation to overcome a bisected TCA cycle and maintain biosynthesis (**Figure 6**). Citrate produced by reductive carboxylation provides a source of OAA to bypass TCA cycle defects, but at the expense of producing massive amounts of lipid. Remarkably, SDH mutant cells have been observed to produce OAA by reverse citrate synthase (82). An increased reliance on PC to support anaplerosis from lactate- or ME-derived pyruvate has also been observed in cells with SDH mutations (23). The PC pathway, though not active in all glutamine-dependent cancers, can be activated when necessary. Attempts to deprive glioblastoma of glutamine-dependent anaplerosis resulted in slowed growth but compensatory activation of PC (28).

Cataplerotic pathways in cancer cells also require unique adaptations to support biosynthesis. Glucose may be metabolized to lactate before reaching tumor tissue (58), which presents a challenge for the biosynthesis of molecules derived from glycolytic intermediates. To meet this challenge, certain cancers have adapted the gluconeogenic enzyme PEPCK (95) to subsidize glycolytic intermediates necessary for the pentose phosphate pathway and the biosynthesis of purines, nucleotides, and lipid esterification, all of which are essential for growth (**Figure 6**). Cataplerosis through PEPCK allowed increased anaplerosis of lactate (95) and glutamine (96) into downstream biosynthetic products, like lipids and ribose (96). Overexpression of *Pck2* in lung cancer supported de novo glycerophospholipid formation, especially of phosphatidylethanolamine, and increased cell growth (83). In contrast, suppressing PEPCK in colon cancer–derived cell lines decreased cell proliferation (96). However, the advantage of PEPCK expression in cancer cells may be specific to contexts where glycolytic intermediates are limiting. In liver and kidney, where PEPCK is very highly expressed, oncogenic transformation suppressed *Pck1* and/or *Pck2* (81, 84). Suppression of PEPCK in liver cancer was associated with decreased survival, enhanced cell growth, and increased tumor recurrence (84). Thus, PEPCK cataplerosis in cancer may be titrated according to the need for glycolytic intermediates, which may be increased in nongluconeogenic tissue and decreased in gluconeogenic tissues, or altogether unnecessary if glycolysis is active. The factors that regulate this metabolic shift remain incompletely understood but are relevant to interventional strategies.

6. SUMMARY

Anaplerosis and cataplerosis provide routes of mass balance for TCA cycle intermediates and allow them to be used in biosynthesis and catabolism without disabling oxidative capacity. Pathways of carboxylation and decarboxylation alter TCA cycle carbon transitions, while other

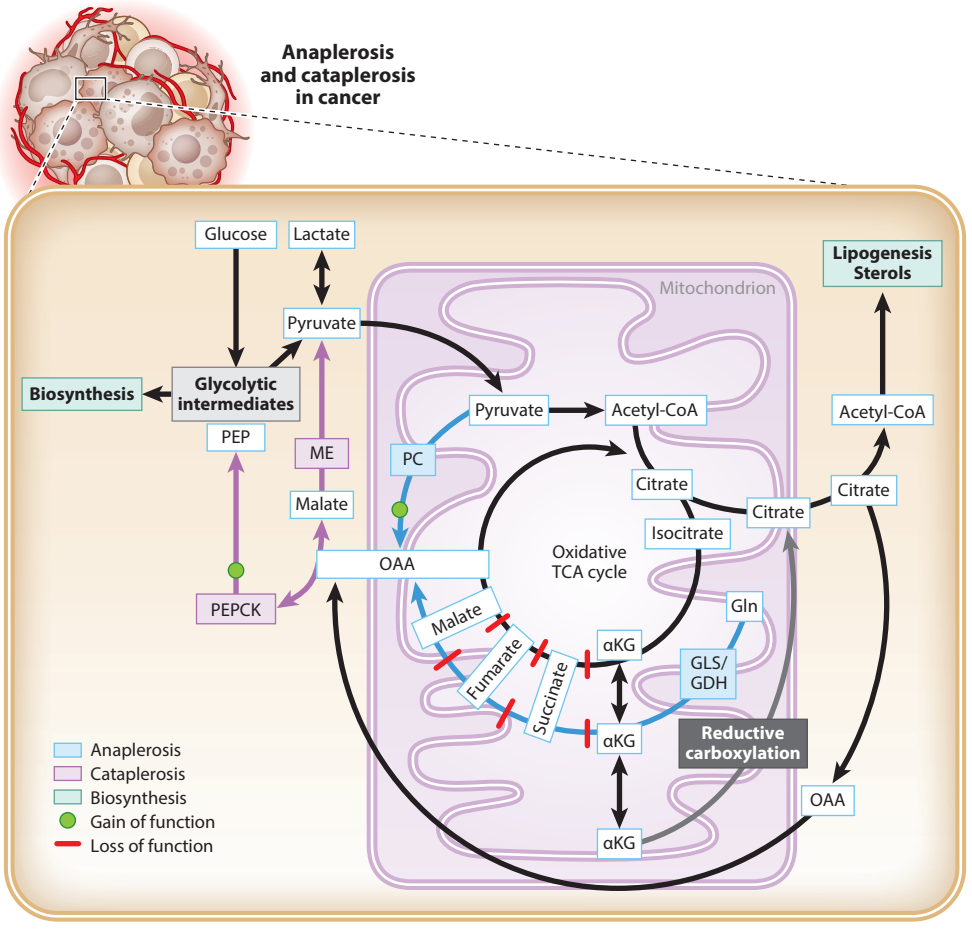

Figure 6

Pathways of anaplerosis and cataplerosis in some cancer cells provide increased metabolic flexibility. Anaplerosis from glutamine is prominent in cancer cells and may overcome reduced redox state and mutations in TCA cycle enzymes (*red bars*). Reductive carboxylation allows αKG to be converted to isocitrate through reverse IDH flux. PC-mediated anaplerosis from lactate and pyruvate allows growth of cancer cells with mitochondrial defects in the generation of OAA. When glycolytic intermediates are scarce, cancers activate cataplerosis through PEPCK, allowing TCA cycle intermediates to support the function of the pentose phosphate pathway and the biosynthesis of purines, nucleotides, and lipids. Abbreviations: GDH, glutamate dehydrogenase; GLS, glutaminase; IDH, isocitrate dehydrogenase; ME, malic enzyme; OAA, oxaloacetate; PC, pyruvate carboxylase; PEP, phosphoenolpyruvate; PEPCK, phosphoenolpyruvate carboxykinase; TCA, tricarboxylic acid; αKG, α-ketoglutarate.

pathways, such as transport shuttles and the urea cycle, exchange intermediates in and out of the cycle without altering carbon transitions. These carbon transitions and dilution of ^{13}C tracers in the TCA cycle can be detected by modern analytical tools, but they require mathematical models to distinguish anaplerotic and oxidative flux. Anaplerotic and cataplerotic sequences facilitate metabolic processes that would otherwise be thermodynamically, compartmentally, or stoichiometrically forbidden. The important role of anaplerosis has been well appreciated since its description by Kornberg (71), but the coordination of these pathways with cellular energy

status, substrate oxidation, and cell signaling is a more recent metabolic paradigm. While intrinsic to classic biochemistry, the fact that anaplerotic and cataplerotic sequences are as necessary for catabolism as they are for biosynthesis is frequently overlooked. Nitrogen trafficking, amino acid oxidation, neurotransmitter recycling, and acid/base balance require these pathways. The dynamic equilibrium of anaplerosis and cataplerosis alters TCA cycle intermediate concentrations and modifies redox state by the mass action of redox-linked dehydrogenase reactions. The array of pathways and functions that overlap with anaplerosis and the TCA cycle must be finely orchestrated, and aspects of this control are frequently dysregulated in metabolic disease. Cancers, more than any other disease, annex anaplerosis and cataplerosis to survive and grow under genetic and nutrient restrictions that would disable normal cell metabolism. Thus, as therapeutic interventions begin targeting pathways that directly or indirectly impinge on the TCA cycle, there is potential for surprising effects in seemingly unrelated pathways. Kornberg's description of anaplerosis in cellular metabolism foreshadowed important roles for TCA cycle intermediates in molecular physiology and disease that will continue to be discovered.

DISCLOSURE STATEMENT

The authors are not aware of any affiliations, memberships, funding, or financial holdings that might be perceived as affecting the objectivity of this review.

ACKNOWLEDGMENTS

The authors are grateful for support from National Institutes of Health grants R01DK078184 (to S.C.B.) and P41EB015908 (to S.C.B. and S.D.), Robert A. Welch Foundation grant I-1804 (to S.C.B.), and the University of Texas Southwestern Center for Human Nutrition. Figures were created with the assistance of BioRender.com.

LITERATURE CITED

1. Adina-Zada A, Zeczycki TN, St. Maurice M, Jitrapakdee S, Cleland WW, Attwood PV. 2012. Allosteric regulation of the biotin-dependent enzyme pyruvate carboxylase by acetyl-CoA. *Biochem. Soc. Trans.* 40:567–72
2. Ajioka RS, Phillips JD, Kushner JP. 2006. Biosynthesis of heme in mammals. *Biochim. Biophys. Acta Mol. Cell Res.* 1763:723–36
3. Alger JR, Sherry AD, Malloy CR. 2018. tcaSIM: a simulation program for optimal design of ^{13}C tracer experiments for analysis of metabolic flux by NMR and mass spectroscopy. *Curr. Metab.* 6:176–87
4. Álvarez Z, Hyroššová P, Perales JC, Alcántara S. 2016. Neuronal progenitor maintenance requires lactate metabolism and PEPCK-M-directed cataplerosis. *Cereb. Cortex* 26:1046–58
5. Alves TC, Pongratz RL, Zhao X, Yarborough O, Sereda S, et al. 2015. Integrated, step-wise, mass-isotopomeric flux analysis of the TCA cycle. *Cell Metab.* 22:936–47
6. Amaral AI, Hadera MG, Tavares JM, Kotter MR, Sonnewald U. 2016. Characterization of glucose-related metabolic pathways in differentiated rat oligodendrocyte lineage cells. *Glia* 64:21–34
7. Antoniewicz MR, Kelleher JK, Stephanopoulos G. 2007. Elementary metabolite units (EMU): a novel framework for modeling isotopic distributions. *Metab. Eng.* 9:68–86
8. Arinze IJ. 2005. Facilitating understanding of the purine nucleotide cycle and the one-carbon pool. Part I. The purine nucleotide cycle. *Biochem. Mol. Biol. Educ.* 33:165–68
9. Battezzati A, Caumo A, Martino F, Sereni LP, Coppa J, et al. 2004. Nonhepatic glucose production in humans. *Am. J. Physiol. Endocrinol. Metab.* 286:E129–35
10. Beale EG, Harvey BJ, Forest C. 2007. *Pck1* and *Pck2* as candidate diabetes and obesity genes. *Cell Biochem. Biophys.* 48:89–95

11. Befroy DE, Perry RJ, Jain N, Dufour S, Cline GW, et al. 2014. Direct assessment of hepatic mitochondrial oxidative and anaplerotic fluxes in humans using dynamic ^{13}C magnetic resonance spectroscopy. *Nat. Med.* 20:98–102
12. Bergman RN, Iyer MS. 2017. Indirect regulation of endogenous glucose production by insulin: the single gateway hypothesis revisited. *Diabetes* 66:1742–47
13. Berndt N, Kolbe E, Gajowski R, Eckstein J, Ott F, et al. 2020. Functional consequences of metabolic zonation in murine livers: new insights for an old story. *Hepatology* 73:795–810
14. Beylot M, Soloviev MV, David F, Landau BR, Brunengraber H. 1995. Tracing hepatic gluconeogenesis relative to citric acid cycle activity *in vitro* and *in vivo*: comparisons in the use of [3-^{13}C]lactate, [2-^{13}C]acetate, and α-keto[3-^{13}C]isocaproate. *J. Biol. Chem.* 270:1509–14
15. Bowtell JL, Marwood S, Bruce M, Constantin-Teodosiu D, Greenhaff PL. 2007. Tricarboxylic acid cycle intermediate pool size: functional importance for oxidative metabolism in exercising human skeletal muscle. *Sports Med.* 37:1071–88
16. Browning JD, Baxter J, Satapati S, Burgess SC. 2012. The effect of short-term fasting on liver and skeletal muscle lipid, glucose, and energy metabolism in healthy women and men. *J. Lipid Res.* 53:577–86
17. Browning JD, Weis B, Davis J, Satapati S, Merritt M, et al. 2008. Alterations in hepatic glucose and energy metabolism as a result of calorie and carbohydrate restriction. *Hepatology* 48:1487–96
18. Burch JS, Marcero JR, Maschek JA, Cox JE, Jackson LK, et al. 2018. Glutamine via α-ketoglutarate dehydrogenase provides succinyl-CoA for heme synthesis during erythropoiesis. *Blood* 132:987–98
19. Burgess SC, Hausler N, Merritt M, Jeffrey FM, Storey C, et al. 2004. Impaired tricarboxylic acid cycle activity in mouse livers lacking cytosolic phosphoenolpyruvate carboxykinase. *J. Biol. Chem.* 279:48941–49
20. Burgess SC, He T, Yan Z, Lindner J, Sherry AD, et al. 2007. Cytosolic phosphoenolpyruvate carboxykinase does not solely control the rate of hepatic gluconeogenesis in the intact mouse liver. *Cell Metab.* 5:313–20
21. Burgess SC, Leone TC, Wende AR, Croce MA, Chen Z, et al. 2006. Diminished hepatic gluconeogenesis via defects in tricarboxylic acid cycle flux in peroxisome proliferator-activated receptor gamma coactivator 1α (PGC-1α)-deficient mice. *J. Biol. Chem.* 281:19000–8
22. Cappel DA, Deja S, Duarte JAG, Kucejova B, Inigo M, et al. 2019. Pyruvate-carboxylase-mediated anaplerosis promotes antioxidant capacity by sustaining TCA cycle and redox metabolism in liver. *Cell Metab.* 29:1291–305.e8
23. Cardaci S, Zheng L, MacKay G, van den Broek NJ, MacKenzie ED, et al. 2015. Pyruvate carboxylation enables growth of SDH-deficient cells by supporting aspartate biosynthesis. *Nat. Cell Biol.* 17:1317–26
24. Cerdán S. 2017. Twenty-seven years of cerebral pyruvate recycling. *Neurochem. Res.* 42:1621–28
25. Chakravarty K, Cassuto H, Reshef L, Hanson RW, Cox MM. 2005. Factors that control the tissue-specific transcription of the gene for phosphoenolpyruvate carboxykinase-C. *Crit. Rev. Biochem. Mol. Biol.* 40:129–54
26. Chen X, Iqbal N, Boden G. 1999. The effects of free fatty acids on gluconeogenesis and glycogenolysis in normal subjects. *J. Clin. Investig.* 103:365–72
27. Chen Z, Tian R, She Z, Cai J, Li H. 2020. Role of oxidative stress in the pathogenesis of nonalcoholic fatty liver disease. *Free Radic. Biol. Med.* 152:116–41
28. Cheng T, Sudderth J, Yang C, Mullen AR, Jin ES, et al. 2011. Pyruvate carboxylase is required for glutamine-independent growth of tumor cells. *PNAS* 108:8674–79
29. Chevalier S, Burgess SC, Malloy CR, Gougeon R, Marliss EB, Morais JA. 2006. The greater contribution of gluconeogenesis to glucose production in obesity is related to increased whole-body protein catabolism. *Diabetes* 55:675–81
30. Clayton PT, Hyland K, Brand M, Leonard JV. 1986. Mitochondrial phosphoenolpyruvate carboxykinase deficiency. *Eur. J. Pediatr.* 145:46–50
31. Consoli A, Kennedy F, Miles J, Gerich J. 1987. Determination of Krebs cycle metabolic carbon exchange in vivo and its use to estimate the individual contributions of gluconeogenesis and glycogenolysis to overall glucose output in man. *J. Clin. Investig.* 80:1303–10

32. Consoli A, Nurjhan N, Reilly JJ Jr., Bier DM, Gerich JE. 1990. Mechanism of increased gluconeogenesis in noninsulin-dependent diabetes mellitus. Role of alterations in systemic, hepatic, and muscle lactate and alanine metabolism. *J. Clin. Investig.* 86:2038–45
33. Cotter DG, Ercal B, Huang X, Leid JM, d'Avignon DA, et al. 2014. Ketogenesis prevents diet-induced fatty liver injury and hyperglycemia. *J. Clin. Investig.* 124:5175–90
34. Crown SB, Ahn WS, Antoniewicz MR. 2012. Rational design of ^{13}C-labeling experiments for metabolic flux analysis in mammalian cells. *BMC Syst. Biol.* 6:43
35. d'Avignon DA, Puchalska P, Ercal B, Chang Y, Martin SE, et al. 2018. Hepatic ketogenic insufficiency reprograms hepatic glycogen metabolism and the lipidome. *JCI Insight* 3:e99762
36. Dai W, Xu L, Yu X, Zhang G, Guo H, et al. 2020. OGDHL silencing promotes hepatocellular carcinoma by reprogramming glutamine metabolism. *J. Hepatol.* 72:909–23
37. DeBerardinis RJ, Lum JJ, Hatzivassiliou G, Thompson CB. 2008. The biology of cancer: Metabolic reprogramming fuels cell growth and proliferation. *Cell Metab.* 7:11–20
38. Deja S, Fu X, Fletcher JA, Kucejova B, Browning JD, et al. 2020. Simultaneous tracers and a unified model of positional and mass isotopomers for quantification of metabolic flux in liver. *Metab. Eng.* 59:1–14
39. Des Rosiers C, Donato LD, Comte B, Laplante A, Marcoux C, et al. 1995. Isotopomer analysis of citric acid cycle and gluconeogenesis in rat liver. *J. Biol. Chem.* 270:10027–36
40. Dozin B, Magnuson MA, Nikodem VM. 1985. Tissue-specific regulation of two functional malic enzyme mRNAs by triiodothyronine. *Biochemistry* 24:5581–86
41. Edgerton DS, Ramnanan CJ, Grueter CA, Johnson KMS, Lautz M, et al. 2009. Effects of insulin on the metabolic control of hepatic gluconeogenesis in vivo. *Diabetes* 58:2766–75
42. Egnatchik RA, Leamy AK, Sacco SA, Cheah YE, Shiota M, Young JD. 2019. Glutamate-oxaloacetate transaminase activity promotes palmitate lipotoxicity in rat hepatocytes by enhancing anaplerosis and citric acid cycle flux. *J. Biol. Chem.* 294:3081–90
43. Ferrannini E, Muscelli E, Frascerra S, Baldi S, Mari A, et al. 2014. Metabolic response to sodium-glucose cotransporter 2 inhibition in type 2 diabetic patients. *J. Clin. Investig.* 124:499–508
44. Fischer H, Esbjörnsson M, Sabina RL, Strömberg A, Peyrard-Janvid M, Norman B. 2007. AMP deaminase deficiency is associated with lower sprint cycling performance in healthy subjects. *J. Appl. Physiol.* 103:315–22
45. Fletcher JA, Deja S, Satapati S, Fu X, Burgess SC, Browning JD. 2019. Impaired ketogenesis and increased acetyl-CoA oxidation promote hyperglycemia in human fatty liver. *JCI Insight* 4:e127737
46. Frederick DW, Loro E, Liu L, Davila A Jr., Chellappa K, et al. 2016. Loss of NAD homeostasis leads to progressive and reversible degeneration of skeletal muscle. *Cell Metab.* 24:269–82
47. Frezza C, Pollard PJ, Gottlieb E. 2011. Inborn and acquired metabolic defects in cancer. *J. Mol. Med.* 89:213–20
48. Friedman B, Goodman EH Jr., Saunders HL, Kostos V, Weinhouse S. 1971. Estimation of pyruvate recycling during gluconeogenesis in perfused rat liver. *Metabolism* 20:2–12
49. Gibala MJ, Young ME, Taegtmeyer H. 2000. Anaplerosis of the citric acid cycle: role in energy metabolism of heart and skeletal muscle. *Acta Physiol. Scand.* 168:657–65
50. Goedeke L, Peng L, Montalvo-Romeral V, Butrico GM, Dufour S, et al. 2019. Controlled-release mitochondrial protonophore (CRMP) reverses dyslipidemia and hepatic steatosis in dysmetabolic nonhuman primates. *Sci. Transl. Med.* 11:eaay0284
51. Gómez-Valadés AG, Méndez-Lucas A, Vidal-Alabró A, Blasco FX, Chillon M, et al. 2008. *Pck1* gene silencing in the liver improves glycemia control, insulin sensitivity, and dyslipidemia in *db/db* mice. *Diabetes* 57:2199–210
52. Groen AK, van Roermund CW, Vervoorn RC, Tager JM. 1986. Control of gluconeogenesis in rat liver cells. Flux control coefficients of the enzymes in the gluconeogenic pathway in the absence and presence of glucagon. *Biochem. J.* 237:379–89
53. Haijes HA, Jans JJM, Tas SY, Verhoeven-Duif NM, van Hasselt PM. 2019. Pathophysiology of propionic and methylmalonic acidemias. Part 1. Complications. *J. Inherit. Metab. Dis.* 42:730–44

54. Hakimi P, Yang J, Casadesus G, Massillon D, Tolentino-Silva F, et al. 2007. Overexpression of the cytosolic form of phosphoenolpyruvate carboxykinase (GTP) in skeletal muscle repatterns energy metabolism in the mouse. *J. Biol. Chem.* 282:32844–55
55. Hasenour CM, Rahim M, Young JD. 2020. In vivo estimates of liver metabolic flux assessed by ^{13}C-propionate and ^{13}C-lactate are impacted by tracer recycling and equilibrium assumptions. *Cell Rep.* 32:107986
56. Homedan C, Laafi J, Schmitt C, Gueguen N, Lefebvre T, et al. 2014. Acute intermittent porphyria causes hepatic mitochondrial energetic failure in a mouse model. *Int. J. Biochem. Cell Biol.* 51:93–101
57. Hughey CC, James FD, Bracy DP, Donahue EP, Young JD, et al. 2017. Loss of hepatic AMP-activated protein kinase impedes the rate of glycogenolysis but not gluconeogenic fluxes in exercising mice. *J. Biol. Chem.* 292:20125–40
58. Hui S, Ghergurovich JM, Morscher RJ, Jang C, Teng X, et al. 2017. Glucose feeds the TCA cycle via circulating lactate. *Nature* 551:115–18
59. Jensen MV, Gooding JR, Ferdaoussi M, Dai XQ, Peterson BS, et al. 2017. Metabolomics applied to islet nutrient sensing mechanisms. *Diabetes Obes. Metab.* 19(Suppl. 1):90–94
60. Jensen MV, Joseph JW, Ronnebaum SM, Burgess SC, Sherry AD, Newgard CB. 2008. Metabolic cycling in control of glucose-stimulated insulin secretion. *Am. J. Physiol. Endocrinol. Metab.* 295:E1287–97
61. Jesinkey SR, Madiraju AK, Alves TC, Yarborough OH, Cardone RL, et al. 2019. Mitochondrial GTP links nutrient sensing to β cell health, mitochondrial morphology, and insulin secretion independent of OxPhos. *Cell Rep.* 28:759–72.e10
62. Jia Y, He J, Wang L, Su L, Lei L, et al. 2018. Dapagliflozin aggravates renal injury via promoting gluconeogenesis in *db/db* mice. *Cell. Physiol. Biochem.* 45:1747–58
63. Jiang W, Wang S, Xiao M, Lin Y, Zhou L, et al. 2011. Acetylation regulates gluconeogenesis by promoting PEPCK1 degradation via recruiting the UBR5 ubiquitin ligase. *Mol. Cell* 43:33–44
64. Jones JG, Naidoo R, Sherry AD, Jeffrey FMH, Cottam GL, Malloy CR. 1997. Measurement of gluconeogenesis and pyruvate recycling in the rat liver: a simple analysis of glucose and glutamate isotopomers during metabolism of [1,2,3-$^{13}C_3$]propionate. *FEBS Lett.* 412:131–37
65. Jones JG, Solomon MA, Sherry AD, Jeffrey FM, Malloy CR. 1998. ^{13}C NMR measurements of human gluconeogenic fluxes after ingestion of [U-^{13}C]propionate, phenylacetate, and acetaminophen. *Am. J. Physiol. Endocrinol. Metab.* 275:E843–52
66. Karaca M, Martin-Levilain J, Grimaldi M, Li L, Dizin E, et al. 2018. Liver glutamate dehydrogenase controls whole-body energy partitioning through amino acid–derived gluconeogenesis and ammonia homeostasis. *Diabetes* 67:1949–61
67. Katz J, Wals P, Lee W. 1993. Isotopomer studies of gluconeogenesis and the Krebs cycle with ^{13}C-labeled lactate. *J. Biol. Chem.* 268:25509–21
68. Kelleher JK. 1986. Gluconeogenesis from labeled carbon: estimating isotope dilution. *Am. J. Physiol. Endocrinol. Metab.* 250:E296–305
69. Koliaki C, Roden M. 2016. Alterations of mitochondrial function and insulin sensitivity in human obesity and diabetes mellitus. *Annu. Rev. Nutr.* 36:337–67
70. Kolwicz SC Jr., Olson DP, Marney LC, Garcia-Menendez L, Synovec RE, Tian R. 2012. Cardiac-specific deletion of acetyl CoA carboxylase 2 prevents metabolic remodeling during pressure-overload hypertrophy. *Circ. Res.* 111:728–38
71. Kornberg H. 1966. Anaplerotic sequences and their role in metabolism. In *Essays in Biochemistry*, ed. P Campbell, G Greville, pp. 1–31. London: Academic
72. Kornberg HL. 1965. Anaplerotic sequences in microbial metabolism. *Angew. Chem. Int. Ed. Engl.* 4:558–65
73. Krebs HA, Hems R, Weidemann MJ, Speake RN. 1966. The fate of isotopic carbon in kidney cortex synthesizing glucose from lactate. *Biochem. J.* 101:242–49
74. Krebs HA, Veech RL. 1969. Equilibrium relations between pyridine nucleotides and adenine nucleotides and their roles in the regulation of metabolic processes. *Adv. Enzyme Regul.* 7:397–413
75. Kucejova B, Duarte J, Satapati S, Fu X, Ilkayeva O, et al. 2016. Hepatic mTORC1 opposes impaired insulin action to control mitochondrial metabolism in obesity. *Cell Rep.* 16:508–19

76. Kumashiro N, Beddow SA, Vatner DF, Majumdar SK, Cantley JL, et al. 2013. Targeting pyruvate carboxylase reduces gluconeogenesis and adiposity and improves insulin resistance. *Diabetes* 62:2183–94
77. Lahey R, Carley AN, Wang X, Glass CE, Accola KD, et al. 2018. Enhanced redox state and efficiency of glucose oxidation with miR based suppression of maladaptive NADPH-dependent malic enzyme 1 expression in hypertrophied hearts. *Circ. Res.* 122:836–45
78. Lambert JE, Ramos-Roman MA, Browning JD, Parks EJ. 2014. Increased de novo lipogenesis is a distinct characteristic of individuals with nonalcoholic fatty liver disease. *Gastroenterology* 146:726–35
79. Landau BR, Schumann WC, Chandramouli V, Magnusson I, Kumaran K, Wahren J. 1993. ^{14}C-labeled propionate metabolism in vivo and estimates of hepatic gluconeogenesis relative to Krebs cycle flux. *Am. J. Physiol. Endocrinol. Metab.* 265:E636–47
80. Latorre-Muro P, Baeza J, Armstrong EA, Hurtado-Guerrero R, Corzana F, et al. 2018. Dynamic acetylation of phosphoenolpyruvate carboxykinase toggles enzyme activity between gluconeogenic and anaplerotic reactions. *Mol. Cell* 71:718–32.e9
81. Lee MH, DeBerardinis RJ, Wen X, Corbin IR, Sherry AD, et al. 2019. Active pyruvate dehydrogenase and impaired gluconeogenesis in orthotopic hepatomas of rats. *Metabolism* 101:153993
82. Lee WD, Mukha D, Aizenshtein E, Shlomi T. 2019. Spatial-fluxomics provides a subcellular-compartmentalized view of reductive glutamine metabolism in cancer cells. *Nat. Commun.* 10:1351
83. Leithner K, Triebl A, Trötzmüller M, Hinteregger B, Leko P, et al. 2018. The glycerol backbone of phospholipids derives from noncarbohydrate precursors in starved lung cancer cells. *PNAS* 115:6225–30
84. Liu MX, Jin L, Sun SJ, Liu P, Feng X, et al. 2018. Metabolic reprogramming by *Pck1* promotes TCA cataplerosis, oxidative stress and apoptosis in liver cancer cells and suppresses hepatocellular carcinoma. *Oncogene* 37:1637–53
85. Luukkonen PK, Dufour S, Lyu K, Zhang XM, Hakkarainen A, et al. 2020. Effect of a ketogenic diet on hepatic steatosis and hepatic mitochondrial metabolism in nonalcoholic fatty liver disease. *PNAS* 117:7347–54
86. Magnusson I, Schumann WC, Bartsch GE, Chandramouli V, Kumaran K, et al. 1991. Noninvasive tracing of Krebs cycle metabolism in liver. *J. Biol. Chem.* 266:6975–84
87. Marin-Valencia I, Roe CR, Pascual JM. 2010. Pyruvate carboxylase deficiency: mechanisms, mimics and anaplerosis. *Mol. Genet. Metab.* 101:9–17
88. Martínez-Reyes I, Chandel NS. 2020. Mitochondrial TCA cycle metabolites control physiology and disease. *Nat. Commun.* 11:102
89. Mazuel L, Blanc J, Repond C, Bouchaud V, Raffard G, et al. 2017. A neuronal MCT2 knockdown in the rat somatosensory cortex reduces both the NMR lactate signal and the BOLD response during whisker stimulation. *PLOS ONE* 12:e0174990
90. McClure WR, Lardy HA. 1971. Rat liver pyruvate carboxylase. *J. Biol. Chem.* 246:3591–96
91. McCommis KS, Chen Z, Fu X, McDonald WG, Colca JR, et al. 2015. Loss of mitochondrial pyruvate carrier 2 in the liver leads to defects in gluconeogenesis and compensation via pyruvate-alanine cycling. *Cell Metab.* 22:682–94
92. McCommis KS, Finck BN. 2019. Treating hepatic steatosis and fibrosis by modulating mitochondrial pyruvate metabolism. *Cell Mol. Gastroenterol. Hepatol.* 7:275–84
93. Mendes AC, Caldeira MM, Silva C, Burgess SC, Merritt ME, et al. 2006. Hepatic UDP-glucose ^{13}C isotopomers from [U-^{13}C]glucose: a simple analysis by ^{13}C NMR of urinary menthol glucuronide. *Magn. Reson. Med.* 56:1121–25
94. Mendez-Lucas A, Duarte JA, Sunny NE, Satapati S, He T, et al. 2013. PEPCK-M expression in mouse liver potentiates, not replaces, PEPCK-C mediated gluconeogenesis. *J. Hepatol.* 59:105–13
95. Montal ED, Bhalla K, Dewi RE, Ruiz CF, Haley JA, et al. 2019. Inhibition of phosphoenolpyruvate carboxykinase blocks lactate utilization and impairs tumor growth in colorectal cancer. *Cancer Metab.* 7:8
96. Montal ED, Dewi R, Bhalla K, Ou L, Hwang BJ, et al. 2015. PEPCK coordinates the regulation of central carbon metabolism to promote cancer cell growth. *Mol. Cell* 60:571–83
97. Moore MC, Cherrington AD, Cline G, Pagliassotti MJ, Jones EM, et al. 1991. Sources of carbon for hepatic glycogen synthesis in the conscious dog. *J. Clin. Investig.* 88:578–87

98. Morken TS, Brekke E, Håberg A, Widerøe M, Brubakk AM, Sonnewald U. 2014. Altered astrocyte-neuronal interactions after hypoxia-ischemia in the neonatal brain in female and male rats. *Stroke* 45:2777–85
99. Mullen AR, Wheaton WW, Jin ES, Chen PH, Sullivan LB, et al. 2011. Reductive carboxylation supports growth in tumour cells with defective mitochondria. *Nature* 481:385–88
100. Murashige D, Jang C, Neinast M, Edwards JJ, Cowan A, et al. 2020. Comprehensive quantification of fuel use by the failing and nonfailing human heart. *Science* 370:364–68
101. Neinast M, Murashige D, Arany Z. 2019. Branched chain amino acids. *Annu. Rev. Physiol.* 81:139–64
102. Neinast MD, Jang C, Hui S, Murashige DS, Chu Q, et al. 2019. Quantitative analysis of the whole-body metabolic fate of branched-chain amino acids. *Cell Metab.* 29:417–29.e4
103. Noack S, Nöh K, Moch M, Oldiges M, Wiechert W. 2011. Stationary versus non-stationary ^{13}C-MFA: a comparison using a consistent dataset. *J. Biotechnol.* 154:179–90
104. Novak CM, Escande C, Gerber SM, Chini EN, Zhang M, et al. 2009. Endurance capacity, not body size, determines physical activity levels: role of skeletal muscle PEPCK. *PLOS ONE* 4:e5869
105. Owczarek A, Gieczewska K, Jarzyna R, Jagielski AK, Kiersztan A, et al. 2020. Hypoxia increases the rate of renal gluconeogenesis via hypoxia-inducible factor 1–dependent activation of phosphoenolpyruvate carboxykinase expression. *Biochimie* 171/172:31–37
106. Owen OE, Kalhan SC, Hanson RW. 2002. The key role of anaplerosis and cataplerosis for citric acid cycle function. *J. Biol. Chem.* 277:30409–12
107. Oz G, Berkich DA, Henry PG, Xu Y, LaNoue K, et al. 2004. Neuroglial metabolism in the awake rat brain: CO_2 fixation increases with brain activity. *J. Neurosci.* 24:11273–79
108. Parker SJ, Metallo CM. 2015. Metabolic consequences of oncogenic IDH mutations. *Pharmacol. Ther.* 152:54–62
109. Peng R, Zhang M, Wang H, Lin J, Wang H, et al. 2020. Advances into understanding the vital role of the mitochondrial citrate carrier (CIC) in metabolic diseases. *Pharmacol. Res.* 161:105132
110. Peoc'h K, Nicolas G, Schmitt C, Mirmiran A, Daher R, et al. 2019. Regulation and tissue-specific expression of δ-aminolevulinic acid synthases in non-syndromic sideroblastic anemias and porphyrias. *Mol. Genet. Metab.* 128:190–97
111. Perry RJ, Camporez JG, Kursawe R, Titchenell PM, Zhang D, et al. 2015. Hepatic acetyl CoA links adipose tissue inflammation to hepatic insulin resistance and type 2 diabetes. *Cell* 160:745–58
112. Pietrocola F, Galluzzi L, Bravo-San Pedro JM, Madeo F, Kroemer G. 2015. Acetyl coenzyme A: a central metabolite and second messenger. *Cell Metab.* 21:805–21
113. Potts A, Uchida A, Deja S, Berglund ED, Kucejova B, et al. 2018. Cytosolic phosphoenolpyruvate carboxykinase as a cataplerotic pathway in the small intestine. *Am. J. Physiol. Gastrointest. Liver Physiol.* 315:G249–58
114. Pound KM, Sorokina N, Ballal K, Berkich DA, Fasano M, et al. 2009. Substrate-enzyme competition attenuates upregulated anaplerotic flux through malic enzyme in hypertrophied rat heart and restores triacylglyceride content: attenuating upregulated anaplerosis in hypertrophy. *Circ. Res.* 104:805–12
115. Previs SF, Brunengraber DZ, Brunengraber H. 2009. Is there glucose production outside of the liver and kidney? *Annu. Rev. Nutr.* 29:43–57
116. Ramnanan CJ, Edgerton DS, Rivera N, Irimia-Dominguez J, Farmer B, et al. 2010. Molecular characterization of insulin-mediated suppression of hepatic glucose production in vivo. *Diabetes* 59:1302–11
117. Rauckhorst AJ, Gray LR, Sheldon RD, Fu X, Pewa AD, et al. 2017. The mitochondrial pyruvate carrier mediates high fat diet–induced increases in hepatic TCA cycle capacity. *Mol. Metab.* 6:1468–79
118. Rebrin K, Steil GM, Mittelman SD, Bergman RN. 1996. Causal linkage between insulin suppression of lipolysis and suppression of liver glucose output in dogs. *J. Clin. Investig.* 98:741–49
119. Roden M, Stingl H, Chandramouli V, Schumann W, Hofer A, et al. 2000. Effects of free fatty acid elevation on postabsorptive endogenous glucose production and gluconeogenesis in humans. *Diabetes* 49:701–7
120. Ryan DG, Murphy MP, Frezza C, Prag HA, Chouchani ET, et al. 2019. Coupling Krebs cycle metabolites to signalling in immunity and cancer. *Nat. Metab.* 1:16–33
121. Samuel VT, Beddow SA, Iwasaki T, Zhang X-M, Chu X, et al. 2009. Fasting hyperglycemia is not associated with increased expression of PEPCK or G6Pc in patients with type 2 diabetes. *PNAS* 106:12121–26

122. Satapati S, Kucejova B, Duarte JA, Fletcher JA, Reynolds L, et al. 2015. Mitochondrial metabolism mediates oxidative stress and inflammation in fatty liver. *J. Clin. Investig.* 125:4447–62
123. Schousboe A, Waagepetersen HS, Sonnewald U. 2019. Astrocytic pyruvate carboxylation: status after 35 years. *J. Neurosci. Res.* 97:890–96
124. Shah AM, Wondisford FE. 2020. Tracking the carbons supplying gluconeogenesis. *J. Biol. Chem.* 295:14419–29
125. Sherry AD, Jeffrey FMH, Malloy CR. 2004. Analytical solutions of ^{13}C isotopomer analysis of complex metabolic conditions: substrate oxidation, multiple pyruvate cycles, and gluconeogenesis. *Metab. Eng.* 6:12–24
126. Sovik O. 1989. Inborn errors of amino acid and fatty acid metabolism with hypoglycemia as a major clinical manifestation. *Acta Paediatr. Scand.* 78:161–70
127. Stark R, Guebre-Egziabher F, Zhao X, Feriod C, Dong J, et al. 2014. A role for mitochondrial phosphoenolpyruvate carboxykinase (PEPCK-M) in the regulation of hepatic gluconeogenesis. *J. Biol. Chem.* 289:7257–63
128. Strisower EH, Kohler GD, Chaikoff IL. 1952. Incorporation of acetate carbon into glucose by liver slices from normal and alloxan-diabetic rats. *J. Biol. Chem.* 198:115–26
129. Stumvoll M, Meyer C, Perriello G, Kreider M, Welle S, Gerich J. 1998. Human kidney and liver gluconeogenesis: evidence for organ substrate selectivity. *Am. J. Physiol. Endocrinol. Metab.* 274:E817–26
130. Sunny NE, Parks EJ, Browning JD, Burgess SC. 2011. Excessive hepatic mitochondrial TCA cycle and gluconeogenesis in humans with nonalcoholic fatty liver disease. *Cell Metab.* 14:804–10
131. Tanaka S, Sugiura Y, Saito H, Sugahara M, Higashijima Y, et al. 2018. Sodium-glucose cotransporter 2 inhibition normalizes glucose metabolism and suppresses oxidative stress in the kidneys of diabetic mice. *Kidney Int.* 94:912–25
132. Thyfault JP, Rector RS. 2020. Exercise combats hepatic steatosis: potential mechanisms and clinical implications. *Diabetes* 69:517–24
133. Titchenell PM, Chu Q, Monks BR, Birnbaum MJ. 2015. Hepatic insulin signalling is dispensable for suppression of glucose output by insulin in vivo. *Nat. Commun.* 6:7078
134. Turer A, Altamirano F, Schiattarella GG, May H, Gillette TG, et al. 2019. Remodeling of substrate consumption in the murine sTAC model of heart failure. *J. Mol. Cell Cardiol.* 134:144–53
135. Utter MF, Keech DB. 1963. Pyruvate carboxylase. I. Nature of the reaction. *J. Biol. Chem.* 238:2603–8
136. Valera A, Pujol A, Pelegrin M, Bosch F. 1994. Transgenic mice overexpressing phosphoenolpyruvate carboxykinase develop non-insulin-dependent diabetes mellitus. *PNAS* 91:9151–54
137. Veech RL, Eggleston LV, Krebs HA. 1969. The redox state of free nicotinamide-adenine dinucleotide phosphate in the cytoplasm of rat liver. *Biochem. J.* 115:609–19
138. Vieira P, Cameron J, Rahikkala E, Keski-Filppula R, Zhang LH, et al. 2017. Novel homozygous *Pck1* mutation causing cytosolic phosphoenolpyruvate carboxykinase deficiency presenting as childhood hypoglycemia, an abnormal pattern of urine metabolites and liver dysfunction. *Mol. Genet. Metab.* 120:337–41
139. Vily-Petit J, Soty-Roca M, Silva M, Raffin M, Gautier-Stein A, et al. 2020. Intestinal gluconeogenesis prevents obesity-linked liver steatosis and non-alcoholic fatty liver disease. *Gut* 69:2193–202
140. Von Glutz G, Walter P. 1976. Regulation of pyruvate carboxylation by acetyl-CoA in rat liver mitochondria. *FEBS Lett.* 72:299–303
141. Wallace M, Metallo CM. 2020. Tracing insights into de novo lipogenesis in liver and adipose tissues. *Semin. Cell Dev. Biol.* 108:65–71
142. Walton ME, Ebert D, Haller RG. 2003. Relative rates of anaplerotic flux in rested and contracted rat skeletal muscle measured by ^{13}C NMR spectroscopy. *J. Physiol.* 548:541–48
143. Wang Y, Kwon H, Su X, Wondisford FE. 2020. Glycerol not lactate is the major net carbon source for gluconeogenesis in mice during both short and prolonged fasting. *Mol. Metab.* 31:36–44
144. Wehbe Z, Tucci S. 2020. Therapeutic potential of triheptanoin in metabolic and neurodegenerative diseases. *J. Inherit. Metab. Dis.* 43:385–91
145. Williams HC, Farmer BC, Piron MA, Walsh AE, Bruntz RC, et al. 2020. APOE alters glucose flux through central carbon pathways in astrocytes. *Neurobiol. Dis.* 136:104742

146. Williamson JR, Kreisberg RA, Felts PW. 1966. Mechanism for the stimulation of gluconeogenesis by fatty acids in perfused rat liver. *PNAS* 56:247–54
147. Yoshino K, Munakata H, Kuge O, Ito A, Ogishima T. 2007. Haeme-regulated degradation of δ-aminolevulinate synthase 1 in rat liver mitochondria. *J. Biochem.* 142:453–58
148. Young JD. 2014. INCA: a computational platform for isotopically non-stationary metabolic flux analysis. *Bioinformatics* 30:1333–35
149. Yuan X, Wang L, Tandon N, Sun H, Tian J, et al. 2020. Triheptanoin mitigates brain ATP depletion and mitochondrial dysfunction in a mouse model of Alzheimer's disease. *J. Alzheimer's Dis.* 78:425–37
150. Zhang W, Bu SY, Mashek MT, OS I, Sibai Z, et al. 2016. Integrated regulation of hepatic lipid and glucose metabolism by adipose triacylglycerol lipase and FoxO proteins. *Cell Rep*. 15:349–59
151. Zhang Y, Taufalele PV, Cochran JD, Robillard-Frayne I, Marx JM, et al. 2020. Mitochondrial pyruvate carriers are required for myocardial stress adaptation. *Nat. Metab.* 2:1248–64